TAMPERE UNIVERSITY OF TECHNOLOGY

BEATRIZ MOLERO RÓDENAS

INFLUENCE OF INTERCELL INTERFERENCE ON HSDPA INDOOR NETWORKS

Master of Science Thesis

Supervisor: M.Sc. Tero Isotalo
Examiner: Prof. Jukka Lempiäinen
Examiners and topic approved in the Faculty of Computing and Electrical Engineering Council meeting on 8 December 2010

ABSTRACT

TAMPERE UNIVERSITY OF TECHNOLOGY
TECHNICAL UNIVERSITY OF MADRID: Master's Degree Programme in Telecommunication Engineering
MOLERO RÓDENAS, BEATRIZ: Influence of intercell interference on HSDPA indoor networks
Master of Science Thesis, 64 pages, 9 Appendix pages
September 2011
Major: Radiocommunications
Supervisor: M.Sc. Tero Isotalo
Examiner: Prof. Jukka Lempiäinen
Keywords: indoor network, intercell interference, other-to-own cell interference ratio, DAS, picocell, HSDPA, WCDMA

Nowadays the high demand of data based services has become one of the key issues in the telecommunications sphere. Mobile cellular networks are thus willing to provide the necessary capacity that this growth demands. While new third generation specifications keep on improving the HSPA and HSPA+ features, a parallel trend trying to provide enough indoor capacity is taking place. The performance of indoor dedicated systems is highly dependent on the interference present in the network.

In this Thesis, the impact of intercell interference on indoor networks is studied. For that purpose, two different measurement campaigns were accomplished in Tampere University of Technology's Tietotalo building. The first of them was held in two small rooms, where picocells and distributed antenna systems (DAS) solutions were tested. The second campaign took place inside a large lecture hall representing an indoor open area, and here diverse picocell layouts were deployed. Analysis took into account interference indicators like signal-to-interference ratio and E_c/N_0, and link adaptation parameters like CQI, modulation usage and transport block size.

This Thesis provides guidelines for indoor planning. It demonstrates that in small rooms, given a fixed number of cells per room, picocells and DAS solutions show similar performance, so picocells are a better option since they require fewer components such as antennas. High-density cell layouts provide higher system TP, but the maximum system TP achievable is dramatically limited by interference. This Thesis also proofs that, in open areas, multicell layouts can give only a marginal increase in system TP with respect to one-cell layouts, and thus multicell configurations are not always needed to be deployed. High-interference regions need to be identified and cleverly located since they degrade the overall system performance and users in those areas experience unbearable low data rates.

PREFACE

This Master of Science Thesis has been written for the completion of my Master of Science Degree in Telecommunication Engineering of the Technical University of Madrid (UPM). The research work has been carried out in the Department of Electrical Engineering at Tampere University of Technology (TUT) during Spring and Summer 2011.

First of all, I would like to express acknowledgments to my examiner Prof. Jukka Lempiäinen and to my supervisor M.Sc. Tero Isotalo for providing me the topic of this thesis. Especial mention to Tero Isotalo for his constant guidance and for his invaluable commitment to my work. I am particularly thankful to PhD. Jarno Niemelä for his always accessible fruitful help and to Rajadurai Subramaniam for his assistance during the measurement campaigns and the proof-reading stage.

Last but not least, I would like to express my gratitude to my boyfriend Juan for his reckless patience and support during the work, and to my sister Verónica and my parents María Paz and José Luis for their unconditional belief in me.

Beatriz Molero Ródenas
beamr9@gmail.com
Tel. +34 680 488435

TABLE OF CONTENTS

LIST OF SYMBOLS

α	Orthogonality factor
γ	Path loss exponent
Δf_c	Coherence bandwidth
η	Load
σ_L	Location variability
Φ	Angle
$\bar{\Phi}$	Mean angle
B	Bandwidth
C	Carrier power
$C_{Shannon}$	Shannon capacity
d	Distance
d_0	Reference distance for the antenna far-field
D	Reuse distance
E_b/N_0	Energy per bit to noise ratio
E_c/N_0	Energy per chip to noise ratio
G	Geometry factor
i	Other-to-own-cell interference
I	Interference power
I_{own}	Intracell interference
I_{other}	Intercell interference
$I_{other\ system}$	Other-system interference
K	Average path loss (unitless constant)
L	Path loss
M	Number of cells per cluster

N	Thermal noise power
$P(\Phi)$	Angular power distribution
P_r	Receive power
P_t	Transmit power
P_{TOT}	Total transmit power of the serving cell
r	Cell radius
R	Data rate
S	Signal power
S_ϕ	Angular spread
S_τ	Delay spread
W	UMTS chip rate

LIST OF ABBREVIATIONS

2G	Second generation
3G	Third generation
3GPP	Third Generation Partnership Project
AMC	Adaptive modulation and coding
BER	Bit error rate
BR	Big Room scenario
BS	Base station
CCCH	Common Control Channels
CDF	Cumulative distribution function
CN	Core network
CQI	Channel-Quality Indicator
DAS	Distributed antenna system
DCH	Dedicated Channel
DL	Downlink
DPCCH	Dedicated Physical Control Channel
DPCH	Dedicated Physical Channel
DPDCH	Dedicated Physical Data Channel
DSCH	Dedicated Shared Channel
EIRP	Effective isotropic radiated power
GSA	Global Mobile Suppliers Association
GSM	Global System for Mobile Communications
HARQ	Hybrid automatic repeat-request
HS	Haroon Shan scenario
HS-DSCH	High-Speed Downlink Shared Channel

HSPA	High-Speed Packet Access
HSPA+	Evolved HSPA
HS-PDSCH	High-Speed Physical Downlink Shared Channel
IM	Interference margin
ISCP	Interference signal code power
MAC	Medium Access Protocol
MAC-hs	High-speed MAC
MC	Measurement campaign
ML	Maximum load
NL	No load
P-CCPCH	Primary Common Control Physical Channel
P-CPICH	Primary Common Pilot Channel
PDU	Protocol Data Unit
PG	Processing gain
QoS	Quality of service
RLC	Radio Link Protocol
RNC	Radio Network Controller
RSCP	Received signal code power
RSSI	Received signal strength indicator
RTT	Round-trip time
SF	Spreading factor
SIR	Signal-to-interference ratio
SNR	Signal-to-noise ratio
TBS	Transport block size
TP	Throughput
TTI	Transmission time interval

UE	User Equipment
UL	Uplink
UMTS	Universal Mobile Telecommunications System
UTRAN	UMTS Terrestrial Radio Access Network
WCDMA	Wideband Code Division Multiple Access

1. INTRODUCTION

Lately, the wireless world has undergone a vast increase in the usage of data based services. The causes behind this spectacular growth might have been based on the popularity of smartphones, on the abundance of wireless device applications and on the flat-rate service plans promoted by operators [1]. This hunger for data traffic has been transmitted to the mobile cellular networks, whose current state is mainly dependent on the data traffic needs. For giving some examples, Vodafone, one of the main operators in Europe, has experienced a growth in data traffic of 300% over the last two years [2]. Furthermore, the trend will continue steadily. According to Cisco's Visual Networking Index update [3], in mobile cellular networks the data traffic growth was more than expected in 2010 and the future growth is predicted to be around 131 % for 2011 and 113 % for 2012. With such a situation, and the consequent overhead of signalling traffic, cellular mobile networks have reached a capacity crunch.

One of the solutions to overcome the capacity problem has been the reckless upgrades and changes in the air interface side of cellular networks. Second generation (2G) systems like Global System for Mobile Communications (GSM) had strong limitations for providing high data rates. This leaded to the introduction in 1999 of a new access technique called Wideband Code Division Multiple Access (WCDMA) and thus conformed a new third generation (3G) system specification called Universal Mobile Telecommunications System (UMTS). However, the theoretical limit of 384 kbps that this technology is capable of was not enough. Later UMTS specifications, from 2005 onwards, tried to give some room to the data traffic needs. According to [4], 99.5 % of 3G operators have already deployed Releases 5 and 6, which means that theoretical downlink peak data rate can reach 14.4 Mbps. Subsequent releases push up the theoretical throughput to 42.2 Mbps if MIMO is used. Finally, new changes in the air interface access technique are coming to the surface with the introduction of fourth generation (4G) systems, namely Long Term Evolution (LTE) networks, that are willing to provide even higher data rates.

Another possibility that soothes the capacity challenge is dedicated indoor solutions. Deploying independent indoor networks offload the outdoor macrocells as well as provide high radio-link quality for indoor users. Indoor planning must take into account the interference management. Despite the fact that indoor cells are smaller

than outdoor ones and consequently use lower transmit power levels, the presence of multiple cells within a limited space creates interference that can degrade the overall system performance. Several studies have been focused on analyzing the gain of having a separate indoor network and also the differences between different indoor dedicated networks [1,5–9]. On the one hand, additional practical results are still required; and on the other hand, there is a lack of information about the effect of intercell interference on different indoor environments (open or small areas) and systems (picocells, DAS, etc.). The scope of this Thesis is to provide guidelines for indoor planning based on the effect that intercell interference has on the behavior of characteristic network parameters like modulation and throughput. For that purpose, diverse measurements were accomplished for different test indoor deployments.

The Thesis is organized as follows. The theoretical basis is presented in chapters 2 to 5. Chapter 2 introduces the main aspects of wireless systems with special focus on interference. Chapter 3 gives the necessary background in WCDMA and UMTS for understanding subsequent sections. In Chapter 4, the main features of the downlink of HSPA and HSPA+ are explained while the particularities of indoor networks are reserved for Chapter 5. The practical work is explained in chapters 6 to 9. Chapter 6 acts as an introduction for the measurement campaigns, Chapter 7 contains the first measurement campaign and Chapter 8 contains the second one. Finally, Chapter 9 gathers the most important conclusions derived from the measurements accomplished.

2. MOBILE COMMUNICATION PRINCIPLES

In the last decades, wireless systems have been widespread all around the world. Communication over fixed radio links has been very common since the first terrestrial radio link was set up in the 1940s [10]. Nowadays, the trend has changed toward achieving full mobility and cellular networks have appeared as one of most liked solutions. This chapter introduces the basic characteristics of mobile cellular systems.

2.1 Propagation concepts of wireless channels

2.1.1 Propagation slope

The propagation slope defines the attenuation between the transmitter and the receiver. In other words, the propagation slope defines how fast signal strength fades as function of distance. E.g., in free space, the attenuation is 20 dB/decade.

A straightforward way of modeling the propagation slope is the *simplified space loss model* [11]:

$$P_r = P_t \cdot K \cdot \left(\frac{d_0}{d}\right)^{\gamma}, \tag{2.1}$$

where P_r and P_t are the received and transmitted power levels, K is a unitless constant that depends on the antenna characteristics and the average channel attenuation, d is the distance from the antenna, d_0 is a reference distance for the antenna far-field, and γ is the path loss exponent.

2.1.2 Fading

Multipath propagation is caused by reflections, diffractions, and scatterings of the signal. Consequently, the signal received is a sum of the original signal plus multiple replicas with different amplitudes and phases. This summation happens in a constructive or destructive way, and thus, causes fast fluctuations in the received signal. This is called fast-fading.

Shadowing, also known as log-normal fading or slow fading, is the variation of the local mean signal level over a wider area. It is caused by large obstructions that impede the propagation path between transmitter and receiver. In outdoors,

buildings, mountains or trees are the cause of slow fading; in indoors, walls and corners have the same role.

The standard deviation of the shadowing distribution is known as the *location variability* σ_L that is usually expressed in decibels. The location variability is highly dependent on the type of environment; for example, it is greater in suburban areas than in open areas [10].

2.1.3 Angular spread

The term angular spread gives the deviation of the signals' incident angle Φ. The angular spread S_ϕ can be calculated as follows [12]:

$$S_\phi = \sqrt{\int_{\bar{\Phi}-180}^{\bar{\Phi}+180} (\Phi - \bar{\Phi})^2 \frac{P(\Phi)}{P_{\Phi total}} d\Phi}, \tag{2.2}$$

where $\bar{\Phi}$ is the mean angle, $P(\Phi)$ is the angular power distribution, and $P_{\Phi total}$ is the total power.

2.1.4 Delay spread and coherence bandwidth

The delay spread S_τ is closely related to multipath. The maximum delay spread is the total time interval between the arrival of the original signal and the arrival of its last significant replica. Normally, the root-mean-square of that total delay spread is given as actual delay spread of the medium.

The coherence bandwidth Δf_c defines the frequency window in which the frequency components of a signal experience fading in a correlated manner. It is inversely proportional to the delay spread S_τ [12]:

$$\Delta f_c = \frac{1}{2\pi S_\tau}. \tag{2.3}$$

If the bandwidth of the system under study is smaller than the coherence bandwidth, then it is a *flat fading* system; on the contrary, if the bandwidth is greater, then the system is *selective fading.*

2.2 Cellular systems

Cellular systems are a type of infrastructure-based network [11]. This means that their structure consist on a centralized coordination of base stations. Those base stations provide access for mobile terminals to a backbone wired network.

2.2.1 The cellular concept

The main difference of cellular networks with regards to other infrastructure-based networks is that one of their main scopes is to provide efficient use of the spectrum by reusing its resources. These resources can be time, frequency, and/or codewords, depending on the type of access technique (Section 2.2.2). Resources are organized in units called channels and different channel sets are assigned to different cells. Cells are controlled by higher entities called base stations and users can move between cells. This process is called *handover*.

Channel sets can be reused again at spatially separated locations and this is called frequency reuse or *channel reuse* [11]. The great benefit of this concept it that it allows a large number of users to be accommodated by taking advantage of the power falloff with distance that signals suffer. The *reuse distance* is the distance between the centers of the cells that use the same channels (Figure 2.1). For simplicity, cells having different channel sets are grouped in clusters. Being M the number of cells per cluster and r the cell radius, the reuse distance D is expressed as follows:

$$D = r\sqrt{3M}. \tag{2.4}$$

Normally, cells are sketched as hexagons. This is a reasonable approximation if propagation follows a simplified path loss model [11]. However, very small cells like indoor cells are closely dependent on the propagation environment; therefore, it is not advisable to approximate their contours with a fixed shape.

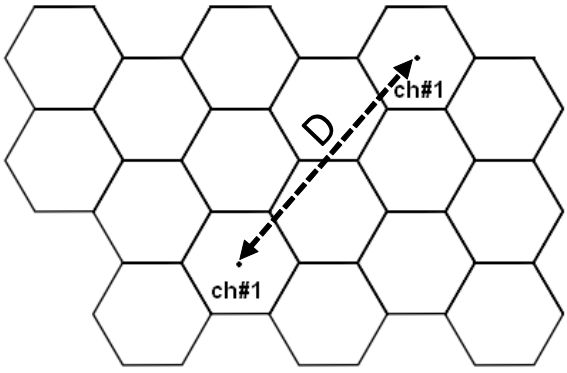

Figure 2.1 *Reuse distance D at hexagonal arrangements of cells.*

The length of the reuse distance has a considerable impact in the performance of the network. The use of small reuse distances increments the number of users that can be serviced by the network because resources can be re-used more often. On the other hand, it increases intercell interference, requires more base stations, and increases the dropping probability [11]. Intercell interference gets higher because

path losses become smaller: for small cells, distance d and propagation exponent γ get smaller [11].

2.2.2 Multiple access techniques

The radio transmission medium has to be shared among all the signals coming from different transmitters within a network. The manner in which this resource is divided in smaller units and given to the different users depends on the multiple access technique under use. Four different access techniques are defined in cellular networks. The paragraphs below describe them.

Frequency Division Multiple Access (FDMA)

This technique divides the total available bandwidth into smaller pieces that are assigned to the users. Each user's spectrum must not overlap with the others and therefore a guard band is added in between.

Time Division Multiple Access (TDMA)

The time axis is organized into frames and slots that are assigned to users. TDMA can only be supported by digital signals due to the transmission discontinuity.

Code Division Multiple Access (CDMA)

In CDMA signals of different users are modulated by orthogonal or quasi-orthogonal spreading codes. Those codes are so called because they enlarge the frequency band that users were using originally. Note that users share the same frequency and time bands. CDMA has a reuse factor of 1, which means that all the codes can be reused in all the cells.

Even if CDMA uses perfectly orthogonal codes, multipath degrades this orthogonality. In consequence, in CDMA systems mutual interference between users is always present, so they are referred as interference-limited systems.

Orthogonal Frequency Division Multiplexing Access (OFDMA)

OFDM is a multicarrier modulation that divides the incoming wideband data stream into multiple narrowband substreams. Each substream occupies a frequency band smaller than the coherence bandwidth and is placed in a orthogonal subcarrier. In this way, a flat-fading environment is simulated. In OFDMA, subsets of those channels are allocated to users.

2.3 High data rates in mobile communications

As it was said in section 2.2.1, cell and cluster sizes, and thus, reuse distance, determines the total capacity. The tradeoff between cell density and interference can be modeled by a parameter called signal-to-interference ratio (SIR). The SIR in a cellular system depends on many factors, like the cell layout and size, reuse distance, and propagation [11]. For better understanding, this is further explained in the sections 2.3.1 and 2.3.2.

2.3.1 Channel capacity in noise-limited scenarios

Given a communication channel, e.g. a radio link, that is only impaired by additive white Gaussian noise (AWGN), then the channel capacity $C_{Shannon}$ is given by the Shannon's equation:

$$C_{Shannon} = B \cdot log_2 (1 + SNR) , \tag{2.5}$$

where B is the bandwidth available for the communication and SNR is the signal-to-noise power ratio (signal power S divided by noise power N).

(2.5) shows the influence of the signal-to-noise ratio (SNR) and the available bandwidth on the maximum achievable data rate: the greater these parameters are, the larger is the capacity. It has been shown [13] that, being the available bandwidth constant, in case of data rates in the same order as or larger than the available bandwidth, any significant increase of the information data rate implies a much larger relative increase in the minimum received signal power.

2.3.2 Influence of interference-limited scenarios

Most commonly, actual mobile-communication systems are interference-limited rather than noise-limited. Specially in the case of dense cell deployments, with several small cells with high traffic load, the *intercell interference* (Section 3.6) is the dominating source of impairment.

Furthermore, the interference can be approximated as Gaussian noise. In the case of a large number of interferers, as in CDMA systems, that method is accurate, but it is not for a small number of interferers, as in TDMA and FDMA systems [11]. Therefore, given the SIR measured at certain cell, (2.5) behaves as the upper bound for cell capacity:

$$C_{Shannon} = B \cdot log_2 (1 + SIR) \leq B \cdot log_2 (1 + SNR) . \tag{2.6}$$

In many respects, the effect of interference can be seen similar to the impact of noise and the conclusions in section 2.3.1 can be developed here:

- The maximum achievable data rate in a given bandwidth is now limited by the SIR and not by the SNR.
- Data rates higher than the available bandwidth would require an un-proportional SIR level. In case of data rates in the same order as or larger than the available bandwidth, any significant increase of the information data rate implies a much larger relative increase in the required SIR [13].

2.3.3 Modulation and coding

Bandwidth is a scarce and expensive resource. Therefore, increasing data rates by means of enlarging the available spectrum band is not always possible. Instead, the usage of higher-order modulations can be a good alternative if high SIR values can be achieved; this is common in small-cell environments with low traffic or in locations close to the antenna site.

Let's consider the modulation schemes used in 3G networks, QPSK, 16QAM and 64QAM. While QPSK allows the transmission of 2 bits per symbol interval, 16QAM gives 4 bits and 64QAM gives 6 bits. That means that, the achievable data rate (bps) and the bandwidth utilization (bps/Hz) is, in 16QAM and 64QAM, two and three times that of QPSK. Constellations of these modulations are depicted in Figure 2.2.

The main drawback was already pointed out in the previous section: higher-order modulations require higher SIR at the receiver for a given bit-error probability, as they provide larger data rates than the available bandwidth.

Finally, higher-order modulations can afford the inclusion of higher coding rates [13]. For example, if we wanted to have a minimum data rate of 2 bits per symbol, QPSK modulation would not give any room for channel-coding, while 16QAM would allow for a channel-coding rate of one third.

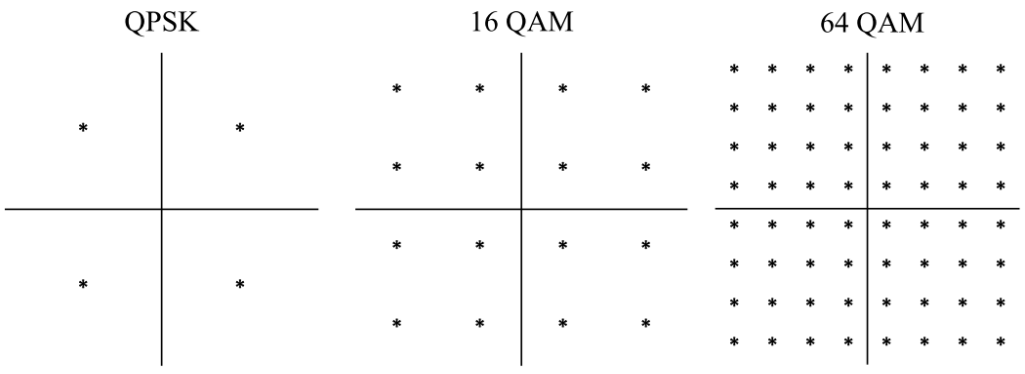

Figure 2.2 *Signal constellations for modulations used in 3G systems.*

3. UMTS OVERVIEW

3.1 What is UMTS? Standardization and spectrum allocation

UMTS is a mobile communications system standardized by the Third Generation Partnership Project (3GPP). 3GPP is a partnership project formed by the standards bodies ETSI (Europe), ARIB/TTC (Japan), CCSA (China), ATIS (North America), and TTA (South Korea) [14]. UMTS is an umbrella term for the third generation radio technologies developed within 3GPP. The last 3GPP specification launched is Release 10, while Release 11 is still in the generation process.

Naturally, switching from 2G to 3G does not only involve changes in the access network but also in the core network. As 3GPP states, UMTS core network becomes "access-agnostic", allowing different ways to connect base stations (BSs) to the core network as for instance with ADSL lines. In the long run, the development of UMTS leads to an all-IP network, which enables a large number of new packet switched services.

The standardization process of UMTS began in the 1990s when 3G research activities were placed at the leading edge while 2G networks were being spread out all around the world. Release 99 was the first specification for UMTS. The access method for the air interface was determined to be WCDMA, with a frequency band allocation of 5 MHz. The first WCDMA networks were launched during 2002 [15]. Later on, Release 5 and Release 6 defined important changes in the air interface with the definition of High-Speed Packet Access (HSPA).

Regarding the spectrum allocation process, the World Administrative Radio Conference (WARC) of the ITU held in 1992 assigned the frequency of around 2 GHz for 3G WCDMA systems. This scheme was adopted by Europe, Asia and most of the Latin American countries. However, North America and some other countries placed 3G near the 2 GHz line, sharing the same frequency bands that 2G operators had already auctioned [16].

3.2 UMTS network architecture (Release 99)

3.2.1 UMTS entities

From a high level perspective, an UMTS network can be divided in three different segments: the User Equipment (UE), the UMTS Terrestrial Radio Access Network (UTRAN) and the core network (CN). The UE interacts with the UTRAN via the air interface Uu. The UTRAN is in charge of handling all the radio-related issues while the CN switches and routes the traffic within the network or towards external networks. It is worth to mention that the structure of the CN of UMTS Release 99 is taken from the GSM specifications, while both UE and UTRAN are completely new [16].

The UE consists of two elements: the Mobile Equipment (ME), which is basically the radio terminal, and the UMTS Subscriber Identity Module (USIM), which is a subscriber identity card.

The UTRAN is formed by two entities explained below. Figure 3.1 sketches the basic UTRAN architecture.

- The *Node B*, also called as base station, has the target of process the air interface physical layer (channel coding, spreading, etc.) as well as performs some basic radio resource tasks. Its functionalities suffer diverse modifications throughout the different releases of UMTS.

- The *Radio Network Controller (RNC)* controls the radio resources and is in charge of several Node Bs. More precisely, a RNC can act as a serving RNC or as a drift RNC. The assignations of these two logical roles change over different releases of UMTS. Roughly, while the serving RNC handles the transport of user data at L2 plane, the drift RNC controls cells used by the mobile terminal [16].

The main elements of R99 CN are [16]:

- The *Mobile Services Switching Center (MSC)* is in charge of switching the circuit-switched (CS) traffic. The Gateway MSC (GMSC) is a MSC connected to an external network

- The *Serving GPRS Support Node (SGSN)* is basically a packet-switched (PS) traffic switcher. The Gateway GPRS Support Node (GGSN) is a SGSN connected to an external network.

- The *Home Location Register (HLR)* is a database that stores important "static" information of the subscriber as for instance acquired services and allowable

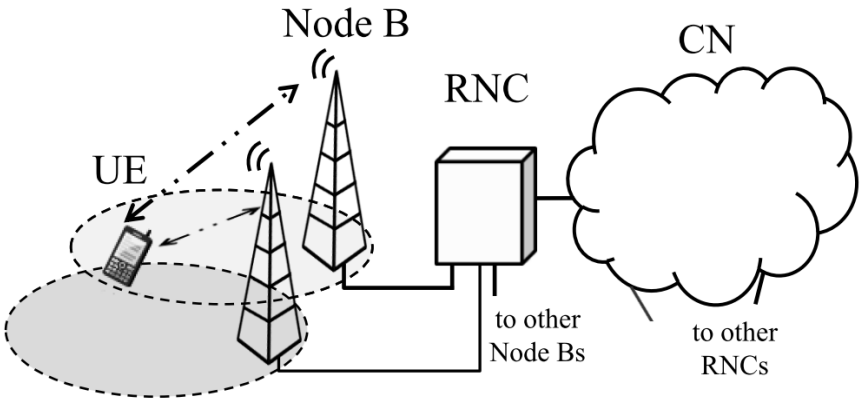

Figure 3.1 *WCDMA radio-access network architecture.*

roaming areas. It participates with the VLR in the UE's mobility procedures by holding information about its location.

- The *Visitor Location Register (VLR)* stores the visiting user's serving profile and location.
- The *Authentication Register (AuC)* is associated with an HLR and stores the authentication keys and the International Mobile Subscriber Identities (IMSI) of the subscribers.

3.2.2 WCDMA protocol architecture

The WCDMA protocol architecture can be seen in Figure 3.2. The three lowest layers are the Radio Link Protocol (RLC), Medium Access Protocol (MAC) and the physical layer, and they are in charge of handling both data and signaling traffic.

The *RLC* is responsible for segmentation of IP packets coming from upper layers into smaller units or Protocol Data Units (PDUs). These RLC PDUs are reassembled in the receiver by the RLC layer. It also handles the automatic repeat-request (ARQ) protocol; the function of ARQ is to request retransmissions when erroneous RLC PDUs are received. The RLC layer is supported in the RNC.

The *MAC* maps the so called logical channels into transport channels. It is also in charge of determining the transport format of the data sent to the physical layer. In each transmission time interval (TTI), one or multiple transport blocks are pushed from the MAC layer to the physical layer. In Release 99, TTI lengths can be 10, 20, 40 or 80 ms, and the MAC layer can vary the transport format between consecutive TTIs. The MAC layer is located in the RNC.

The *physical layer* performs coding, interleaving, multiplexing, spreading and modulation. It is mainly situated in the Node B. A transport block is the basic unit

of data exchange between MAC and physical layer, and its length in bits is called transport-block size (TBS).

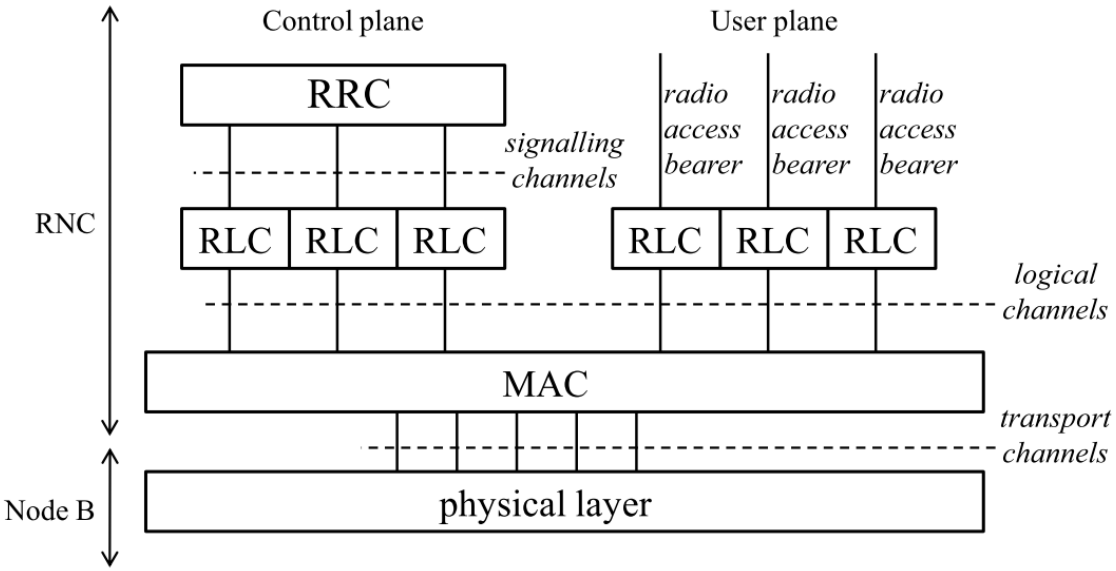

Figure 3.2 *WCDMA protocol architecture [13].*

3.3 General characteristics of WCDMA

WCDMA is a Direct-Sequence Code Division Multiple Access (DS-CDMA) system. The principle of such a system is that the user information is spread over a wide bandwidth by means of pseudo-random sequences of chips. In fact, in WCDMA the chip rate is 3.84 Mcps, which leads to a carrier bandwidth of around 5 MHz.

Most commonly, two different carriers of 5 MHz are used for downlink and uplink transmissions, concept that is referred as Frequency Division Duplex (FDD) mode. Some realizations of UMTS use Time mode (TDD) operation, which means that only one carrier is used for both directions of the communication.

3.3.1 Spreading and scrambling

Spreading and scrambling are two operations that occur one after the other in WCDMA systems. *Spreading* is the first step and its aim is to enlarge the spectrum usage up to 5 MHz by means of different spreading or channelization codes. Channelization codes separate transmissions from a singles source: in the downlink, they discriminate between connections within one sector; in the uplink, they distinguish between the dedicated channels established with one terminal.

The spreading codes used in UMTS are Orthogonal Variable Spreading Factor

(OVSF) type, fact that leads to good orthogonality properties between code sequences and possibility of using variable spreading factor. Spreading Factor (SF) can be defined as the number of chips used for each data bit and is expressed as follows:

$$SF = \frac{W}{R}, \tag{3.1}$$

where W is the chip rate (3.84 Mcps) and R is the bit rate.

OVSF codes are arranged in trees that means that in UMTS all the users of one cell share the same tree. The lower the spreading factor is, the more code resources are being consumed by the channel holding that spreading factor.

Moving forward, the second step of the UMTS coding is *scrambling*. While spreading separate different transmissions within one source, scrambling separates different sources. It is used in the downlink for distinguishing base stations and in the uplink for differentiating mobile terminals. Unlike spreading, scrambling does not spread the signal.

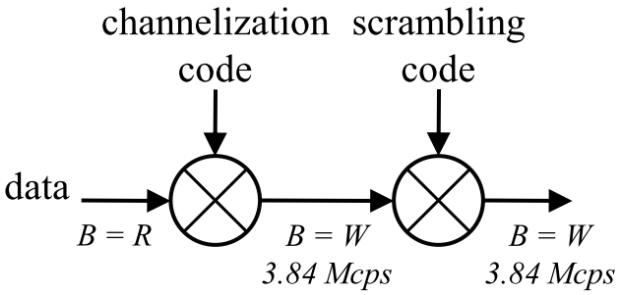

Figure 3.3 *Spreading and scrambling in WCDMA systems.*

3.3.2 Power control

Power control is a term that gathers different procedures related to the adjustment of power levels in a UMTS network. The most outstanding one in terms of impact on the WCDMA system's performance is the so called *fast closed-loop power control*.

Closed-loop power control in the uplink copes with the near-far problem of WCDMA-based networks. This situation refers to the fact that, without any power adjustment, transmissions from terminals close to the base station could mask transmissions from terminals further away. Uplink fast power control is performed 1500 times per second, so it operates faster than the majority of the path changes.

Fast power control operates as follows. The base station estimates the SIR of every mobile and compares it with a target SIR. If it is higher, the base station commands the mobile to low the power; if the measured SIR is smaller than the

target SIR, then the base station commands the mobile to increase the power [16].

Regarding the downlink direction, fast closed-loop power control is used here as well, although not primarily motivated by the near-far problem [13]. On the contrary, it is mainly motivated by the presence of fast-fading. This can be overcome by varying the transmission power: when the channel conditions are favorable, less transmission power is used and viceversa. This typically results in a lower average transmitted power so reducing the average intercell interference and thus, increasing system capacity.

3.3.3 Softer and soft handovers

Another of the benefits of the spreading and scrambling techniques inherent to WCDMA is the possibility of performing soft and softer handovers.

In the downlink, transmissions from different cells or sectors, whether if they belong to the same base station or not, use different codes. This allows the mobile terminals located in the overlapping area between two cells/sectors to use concurrent air physical channels from both cells/sectors. If the sectors belong to the same base station, then the technique is called softer handover. If they do not, then the mobile terminals are in soft handover.

Similarly, in the uplink different UE's transmissions are code characterized, and therefore signals belonging to one terminal but coming from different cells can be combined.

Since in softer handovers the sectors that create the overlapping area belong to the same base station, the combining is done at this entity. On the contrary, in soft handovers the combining is performed at the RNC [16].

3.4 Main measurement concepts of UMTS networks

3.4.1 RSCP, RSSI and ISCP

Received signal code power (RSCP) and *received signal strength indicator (RSSI)* are power levels measured by the UE being the antenna connector the reference point. The RSCP is the received power on one code of one particular desired physical channel; in FDD mode, this channel is the Primary Common Pilot Channel (P-CPICH). RSCP acts as a coverage indicator.

The RSSI is the total received wideband power; it includes interference power, thermal noise and noise generated in the receiver, within the bandwidth defined by the receiver pulse shaping filter. As in the case of RSCP, RSSI levels are measured on the downlink carrier [17].

The concept of *interference signal code power (ISCP)* is similar to the RSSI's

definition, but with some subtle differences. ISCP is the interference on the received signal measured on the pilot bits. Only the nonorthogonal part of the interference is included in the measurement.

3.4.2 SIR and E_c/N_0

The similarities and differences that could be between E_c/N_0 and SIR definitions are parallel to those between RSSI and ISCP.

E_c/N_0 is the received energy per chip divided by the power density in the band. E_c/N_0 is calculated as the ratio between RSCP and RSSI [17] and in consequence related measurements shall be performed on the P-CPICH. E_c/N_0 is used as a coverage quality indicator [6].

$$E_c/N_0 = \frac{RSCP}{RSSI}. \tag{3.2}$$

While E_c/N_0 is a parameter measured by the UE, SIR is a measurement ability of both UTRAN and UE. Again, the reference point is the antenna connector. Interference level is indicated with SIR of the P-CPICH and is defined as [6]

$$SIR_{P-CPICH} = SF_{256}\frac{\frac{P_{P-CPICH}}{L}}{\frac{P_{TOT}}{L}(1-\alpha) + I_{other} + N}, \tag{3.3}$$

where SF_{256} is the processing gain for P-CPICH, $P_{P-CPICH}$ is the transmit power of P-CPICH, P_{TOT} is the total transmit power of the serving base station, I_{other} is the intercell interference power, N is the received noise power, α is the orthogonality factor, and L is the path loss between the serving base station and the terminal.

3.4.3 Processing gain

The definition of processing gain (PG) is equivalent to the Spreading Factor (SF) expression, they are synonyms, but normally PG is expressed in logarithmic scale:

$$PG\ (dB) = 10 \cdot log_{10}\left(\frac{W}{R}\right). \tag{3.4}$$

The term *gain* refers to gain achieved in the despreading process at the receiver as it can sum coherently the multipath copies of the original signal.

3.4.4 E_b/N_0

Unlikely E_c/N_0, E_b/N_0 is calculated after the despreading process. Therefore, both terms are related by the PG in logarithmic scale:

$$E_b/N_0 \ (dB) = E_c/N_0 \ (dB) + PG \ (dB). \tag{3.5}$$

This term is highly important because of its close relation with bit-error rate (BER) and its application for setting quality targets in UMTS networks.

3.5 Link budget and link parameters

3.5.1 Definition of link budget

The so called *power budget* or *link budget* is a procedure that is part of the radio network planning process. WCDMA radio network planning is divided in three steps: dimensioning, coverage and capacity planning and optimization; the link budget calculations belong to the first one [18].

The aim of the link budget calculations is to get a rough estimate of the cell range. These issues are shortly explained in this section because of its didactic value. Finally, a link budget can be sectioned in three parts: the transmitting end, the receiving end and the RF channel.

3.5.2 The transmitting end

The contribution of the transmitting end to the link budget is the *effective isotropic radiated power (EIRP)* that is the radiated power at the very end of the transmitter.

3.5.3 The receiving end

The receiving end adds to the link budget the *required signal level* concept. This is the power level that the receiver needs as minimum for guaranteeing a particular quality of service (QoS), taking as reference point the end of the antenna line.

$$\begin{aligned} \textit{Required signal level (dBm)} = {} & \textit{Receiver sensitivity (dBm)} \\ & - \textit{RX antenna line gains (dB)} \\ & + \textit{RX antenna line losses (dB).} \end{aligned} \tag{3.6}$$

At this point, it is worth to remind the presence of an E_b/N_0 requirement for the UMTS service type under study. Consequently, the *receiver sensitivity* threshold must fulfill [16]:

$$\begin{aligned} \textit{Receiver sensitivity (dBm)} &= \textit{C/I (dB)} + \textit{Total interference (dBm)} \\ &= E_b/N_0\,(dB) - \textit{PG (dB)} \\ &+ \textit{Total interference (dBm).} \end{aligned} \tag{3.7}$$

In Equation 3.7, C and I form the carrier-to-interference power ratio C/I and the term *Total interference* consists of two contributions: the *received noise power*, which is the receiver thermal noise stressed by the noise figure; and the *interference margin (IM)*. Interference is taken into account in the link budget because it affects the coverage radius. As the interference margin is added to the noise floor, this parameter is also called *UMTS noise increase* [19].

3.5.4 The RF channel

For making up the cell range, the final *maximum path loss* value is needed. This is expressed as follows:

$$\begin{aligned} \textit{Maximum path loss (dB)} &= \textit{EIRP (dB)} - \textit{Required signal power (dBm)} \\ &- \textit{total fading margin (dB)} + \textit{handover gain (dB).} \end{aligned} \tag{3.8}$$

The EIRP and required signal power parameters have been already explained in this section.

The *total fading margin* is the summation of the slow-fading and the fast-fading margins plus the losses inherent to penetration of buildings, cars and people at the receiver end. The *log-normal or slow-fading margin* is the margin required to provide coverage availability considering the presence of slow-fading in the system. It is defined at the cell edge of individual cells [18].

The *fast fading margin* is also called *power control headroom* and is a characteristic parameter of UMTS networks. The utilization of closed loop fast power control in WCDMA systems requires the addition of some power headroom at the base station side [16].

The *handover gain* is the gain that handovers -soft or hard- give against slow fading. In case of multiple base stations, the probability to experience outage from two base stations is smaller than the resulting outage probability of a single-cell situation [18]. This issue can be expressed as a gain in the link budget.

Finally, there is a last component of the link budget, the *soft handover diversity gain*. The soft handover diversity gain is included in traditional macro link budgets, typical using 3 dB. The users on the edge of the cell are in soft handover, which

means that they use macro diversity techniques that improve the overall link. Some publications have reported that this gain should not be considered in most of the cases [19], and even some others [16, 18, 20] does not take it into account in the link budget calculations.

3.6 Load and interference

Interference occurs in UMTS networks since all transmissions share the same frequency band and the codes separating channels, users and base stations, are not fully orthogonal. There are two types of interference: intracell and intercell interference. The total interference I_{total} is the sum of intracell interference I_{own}, intercell interference I_{other}, as well as other-system interference $I_{other\ system}$ and thermal noise N [21].

$$I_{total} = I_{own} + I_{other} + I_{other\ system} + N. \tag{3.9}$$

Uplink intracell interference is the sum of the WCDMA uplink signals of all the users communicating with the Node B cell. Also, it includes the multipath components of the each user's transmitted waveform. It is worth to mention that first, a non-zero cross-correlation exists between each user's scrambling code, and second, multipath degrades even more orthogonality. Regarding *uplink intercell interference*, this is the sum of all the users' signals that do not communicate with the base station under consideration. The source of such interference is those other-cell terminals cannot be power controlled by the own Node B [22].

Downlink interference appears because the spreading codes are not idelly orthogonal. According to [23], downlink interference levels are high even if cell load is low, because the BSs always have to transmit the DL common channels.

Interference has two main effects in the performance of the victim cell: on the one hand, it sums to the noise floor; on the other hand, it generates an increase in the cell load. Actually, the capacity of a UMTS network is interference-limited, which means that a rise in interference in a cell can cause blocked calls [12]. A load curve characterizes the relationship between the cell load η and the interference IM, for both uplink and downlink ((3.12) and (3.14)).

The parameter little i

The other-to-own cell interference i, also called little i, is the ratio between the intercell interference I_{other} and the intracell interference I_{own}.

$$i = \frac{I_{other}}{I_{own}}. \tag{3.10}$$

In the UL, little i is the other cell to own cell interference ratio seen by the

base station receiver. In the DL, little i corresponds to the ratio of other cell to own cell base station power. Each user sees a different DL i, depending on its location in the cell. The explanation comes straight when thinking over the intercell component of little i: terminals close to the cell edge may experience higher interference coming from surrounding cells that terminals near the base station. Furthermore, the other-to-own cell interference depends on the propagation environment, cell density and traffic profile. For an instance, typical values of little i in indoor picocell based scenarios are between 0.1 and 0.2 while in macrocell based cases is around 0.5 [21].

Uplink load equation

For the uplink (UL) direction, two equations (3.11) and (3.12) express the relation between load and interference:

$$\eta_{UL} = \sum_{j=1}^{N} \frac{1}{1 + \frac{W}{(E_c/N_0)_j \cdot R_j \cdot \upsilon_j}} (1 + i)\,. \tag{3.11}$$

where η_{UL} is the uplink load, N is the number of active users in the cell, W is the UMTS chip rate (3.84 Mcps) and R_j, $(E_b/N_0)_j$ and υ_j, are the bit rate, E_b/N_0 requirement and activity factor of the jth user [12]. Note that for the uplink, the total load is the contribution of the loads of all the users. Finally, the most outstanding term for our study is the other-to-own cell interference (little i), which multiplies the whole summation of single-user loads.

$$IM_{UL} = -10log(1 - \eta_{UL}), \tag{3.12}$$

where IM_{UL} is the required uplink IM that has to be added to the noise floor. In other words, load causes a noise increase.

Downlink load equation

Like for the UL, for the downlink (DL) direction, two equations (3.13) and (3.14) express the relation between load and interference. The DL load equation has similar components as in the UL load equation, except for the orthogonality factor α_j. Its 0-to-1 possible value depends on the orthogonality of the codes used. Since multipath impairs that orthogonality, α is highly dependent on the type of environment (macro, micro or picocellular, outdoor or indoor). As a matter of fact, in indoor the delay spread rarely exceeds a few hundred nanoseconds, so α values are normally closer to 1 than in outdoors (an orthogonal factor of 0.85 is typically used in indoor link budgets [12, 21]).

$$\eta_{DL} = \sum_{j=1}^{N} \upsilon_j \frac{(E_b/N_0)_j}{\frac{W}{R_j}} \left[(1-\alpha_j) + i_j\right], \tag{3.13}$$

$$IM_{DL} = -10log(1-\eta_{DL}). \tag{3.14}$$

It can be seen in (3.11) and (3.12), that the more users are in the network, the more interference is present. Actually, the downlink load factor η_{DL} can be understood as the increase in the required base station power in order to maintain the N connections [16].

3.7 Physical and transport channels

3.7.1 User data transmission

Downlink Dedicated Channels

There are two types of downlink dedicated channels: the dedicated physical channel (DPCH) and the physical downlink shared channel (PDSCH). The downlink DPCH consist of two physical channels that are multiplexed in time: the downlink Dedicated Physical Data Channel (DPDCH) and the Dedicated Physical Control Channel (DPCCH).

The *downlink DPDCH* carries user data from the Node B to the UE. The *downlink DPCCH* carries signalling information regarding three different aspects: pilot bits for the decoding of the data channel DPDCH, power control messages, and the field Transport Format Combination Indicator (TFCI) describing the structure of the modulated data.

In the downlink Dedicated Physical Channel (DPCH), the spreading factors range from 512 to 4 and some restrictions exist in the use of spreading factor (SF) 512 when the terminal is in soft handover [16]. The modulation used is QPSK. It is also possible to allocate multiple downlink DPCHs to the same user (multicode operation), but each with a different channelization code [21].

(3.15) gives the way of calculating the final data rate R considering the modulation and coding schemes used [16].

$$R = \frac{W}{SF} \cdot \textit{modulation order} \cdot \textit{coding rate} \cdot \textit{number of codes}. \tag{3.15}$$

Finally, the *PDSCH* is a channel that can be shared by multiple users. It carries high rate data when the transmissions are infrequent.

Uplink dedicated Channels

The uplink directions presents two dedicated channels: the *uplink DPDCH* and the *uplink DPCCH*. They perform similar functionalities than those in the downlink direction. The main difference is that they are code multiplexed rather than time multiplexed. Furthermore, the uplink DPCCH carries feedback information when closed-loop transmit diversity is used [16]. Another difference is that the uplink DPCCH always uses a 256-spreading code and the DPDCH's spreading factor ranges from 256 to 4.

Multicode transmission is supported too, with UEs able to transmit up to six DPDCHs. However, in case of multicode operation, channelization codes cannot use a SF exceeding 16 [21].

Modulation is a fixed parameter and BPSK modulation is used in the UL data channel. On the contrary, the SF can change on a frame-by-frame basis, and so does it the data rate.

Equation 3.15 gives the way of calculating the final data rate R considering the modulation and coding schemes used. Table 3.1 shows the minimum and maximum reachable data rates in UMTS R99 for both uplink and downlink directions [16].

Table 3.1 *Maximum and minimum data rates at UMTS R99.*

	Spreading Factor (SF)	DPDCH bit rate	Max. user data rate with 1/2 coding
Uplink (max. SF)	256	15 kbps	7.5 kbps
Uplink (min. SF)	4 with 6 parallel codes	5740 kbps	2.8 Mbps
Downlink (max. SF)	512	3-6 kbps	1-3 kbps
Downlink (min. SF)	4 with 3 parallel codes	5616 kbps	2.8 Mbps

The dedicated and shared transport channels DCH and DSCH

The *Dedicated Channel (DCH)* is the only dedicated transport channel. It can be a DL or UL channel and is mapped onto the physical channels already mentioned PDDCH and PDCCH. It carries user data as well as control information from higher layers. Important features of this transport channel is that it supports soft-handover operation, allows variable data rates (variable SF) in a frame-by-frame basis and is fast power-controlled. The Dedicated Channel (DCH) appears in all the releases of UMTS.

Unlikely the DCH, the *Dedicated Shared Channel (DSCH)* is a downlink transport channel that is mapped on the PDSCH. A DSCH is always associated with a DCH

and can carry user data and/or control information from higher layers [16].

3.7.2 Signalling

Common Pilot Channel (CPICH)

The common pilot channel is an unmodulated channel whose aim is to help the channel estimation at the UE. It is scrambled with the cell's characteristic scrambling code and uses the spreading factor of 256. There is only one primary CPICH per cell. It does not carry any higher layer information and is specially important for the measurements concerning cell reselections.

Synchronization Channel (SCH)

The synchronization channel is used for cell search. There are two types of SCH, primary SCH and secondary SCH. It is the secondary SCH that gives information about the group of cells the terminal belongs to.

Primary Common Control Physical Channel (P-CCPCH)

The P-CCPCH is the physical channel carrying the Broadcast Channel (BCH). As it needs to be demodulated by all the terminals in the system, it has fixed rate and constant channelization code (256), as well as relatively high power.

The Broadcast Channel (BCH) is a transport channel used to transmit information specific to a cell's UTRA, like possible random access codes, access slots, etc [16].

4. HSPA DOWNLINK EVOLUTION: FROM RELEASE 5 ONWARDS

4.1 Evolution and architecture of HSPA

4.1.1 3GPP specifications

Release 99 lacked of an efficient channel for the carrying of packet traffic. The DCH was inappropriate for bursty and high-data rate services due to its high channel reconfiguration time. The DSCH showed up as a better channel for that kind of services, but still some improvements needed to be performed [24].

The first HSPA specification appeared in UMTS Release 5, with the definition of new features for the downlink. Lately, Release 6 specified the uplink of HSPA and added some modifications to the downlink of HSPA. The aim of HSPA was on the one hand, to cope with the increasing demand of higher data rates; and on the other hand, to overcome the restrictions that Release 99 exhibited when handling different service classes. The downlink of HSPA is well known as HSDPA.

Evolved HSPA (HSPA+) appeared at Release 7 as the natural evolution to HSPA; the downlink of HSPA+, also called as HSDPA+, doubles the data capacity of HSPA and more than doubles the voice capacity of WCDMA. This thesis only covers the downlink of the technologies HSPA (Release 6) and HSPA+ (Release 7).

Finally, later 3GPP specifications added new upgrades to HSPA+. Release 8 introduced the dual-carrier capability, aggregating two 5 MHz carriers. Release 9 defined the multicarrier operation in the 10 MHz band. Finally, HSPA+ Release 10 supports aggregation of 4 carriers (20 MHz) in the downlink, offering a theoretical 168 Mbps peak data rate.

According to the figures reported by the Global Mobile Suppliers Association (GSA) in June 2011 [4], 99.5 % of 3G operators have already deployed HSPA and around 31 % of those networks are HSPA+.

4.1.2 HSPA architecture

The change towards a flat architecture begins with HSPA. Several functionalities are transferred from the RNC to the Node B. In HSPA, the differences between serving RNC and drift RNC (Section 3.2.1) disappear [15].

HSDPA adds a new sublayer, the MAC-hs, in the Node B. Its duties are scheduling of HSPA dedicated channels, rate control and handling of retransmissions. Thus, the Node B, which before was mainly in charge of power control related issues, is now conferred layer 2 capabilities. The MAC layer functionalities of HSPA can operate independently of DCH operation of Release 99 [15]. In this way, the RNC retains only the management of mobility and resources as well as the traffic control functionalities.

In Release 7 (HSPA+), all the RNC's functionalities can be moved to the Node B and the SGSN can be connected directly to each base station. The so-called *direct tunnel* solution makes the SGSN transparent to the user data traffic, regardless the presence or not of RNC [25].

4.2 New channels

4.2.1 High-speed downlink shared channels

A key feature of the evolution of the WCDMA downlink towards HSDPA is the shared channel transmission. The shared channel of Release 99, the DSCH, was removed from the 3GPP specifications from Release 5 onwards. One of the advantages of the old DSCH was that it could be shared by the users in a time-domain manner, being more suitable for bursty high-speed data traffic. The new HSDPA High-Speed Downlink Shared Channel (HS-DSCH) has this same capability.

The *High-Speed Downlink Shared Channel (HS-DSCH)* is a transport channel that has a fixed SF of 16 and corresponds to a set of channelization codes whose number is configurable between 1 and 15. In other words, there are 1-to-15 *High-Speed Physical Downlink Shared Channels (HS-PDSCHs)* available to allocate between users.

The HS-DSCH can be shared in time domain or in code domain (Figure 4.1). Most of the times, terminals are not 15-codes capable and/or the data transmission does not require the full set of 15 physical channels. In those conditions, it is more beneficial to allocate subsets of codes to every user and so does the HS-DSCH. The allocation of codes is done on 2 ms TTI basis. Note that the TTI is shorter that in Release 99. This results in a more rapid allocation of the shared resources. The main differences between the data channels of WCDMA Release 99 and the HS-DSCH are shown in Table 4.1.

In Release 7, some modifications are made on the HS-DSCH. With MIMO (Section 4.4.2), two orthogonal streams can be transmitted simultaneously in HSPA+. The HS-DSCH is made capable of supporting up to two transport blocks per TTI, where each transport block represents one stream [13].

The downlink control signaling is carried on the *High-Speed Shared Control Channel (HS-SCCH)*. The HS-SCCH is always transmitted in parallel to the HS-DSCH.

Table 4.1 *Differences between Release 99 channels and the HS-DSCH of Release 7 [13,25].*

Release	R99	R99	R7
Feature	DSCH	DCH	HS-DSCH
Variable SF	Yes (4-256)	Yes (4-512)	No (16)
Fast power control	Yes	Yes	No
AMC	No	No	Yes
Fast L1 HARQ	No	No	Yes
Multicode operation	Yes	Yes	Yes, extended
TTI	10 or 20 ms	10, 20, 40 or 80 ms	2 ms
Location of MAC	RNC	RNC	Node-B
Soft handover	Yes	Yes	No
Modulation	QPSK	QPSK	QPSK, 16QAM or 64QAM

It informs about the code tree, the modulation and the transport block size used, as well as the user/s being scheduled. Each HSPA terminal must be capable of monitoring up to four HS-SCCHs; four HS-SCCH has been found to be suitable for the scheduling of multiple HSPA UEs [26]. Neither the HS-PDSCH, nor the HS-SCCH, can support soft handover in HSDPA. The limitation arises because of the location of the scheduling at Node B.

Finally, as in the HS-DSCH case, the HS-SCCH undergoes some changes when upgrading to HSPA+. Its format is modified so that it can give information about the number of streams and the modulation and coding schemes used in each one [13].

4.2.2 The High-Speed Dedicated Physical Control Channel

Downlink HSDPA transmissions require some feedback channel to support hybrid automatic repeat-request (HARQ) and quality reports. This is performed by the uplink High-Speed Dedicated Physical Control Channel (HS-DPCCH). This physical channel has two main responsibilities. First, for each TTI in which the UE has been scheduled in downlink, the HS-DPCCH carries an ACK or NAK indicating the success or failure of the HS-DSCH decoding. Second, it transmits a Channel-Quality Indicator (CQI) that informs the base station about the instantaneous DL channel conditions.

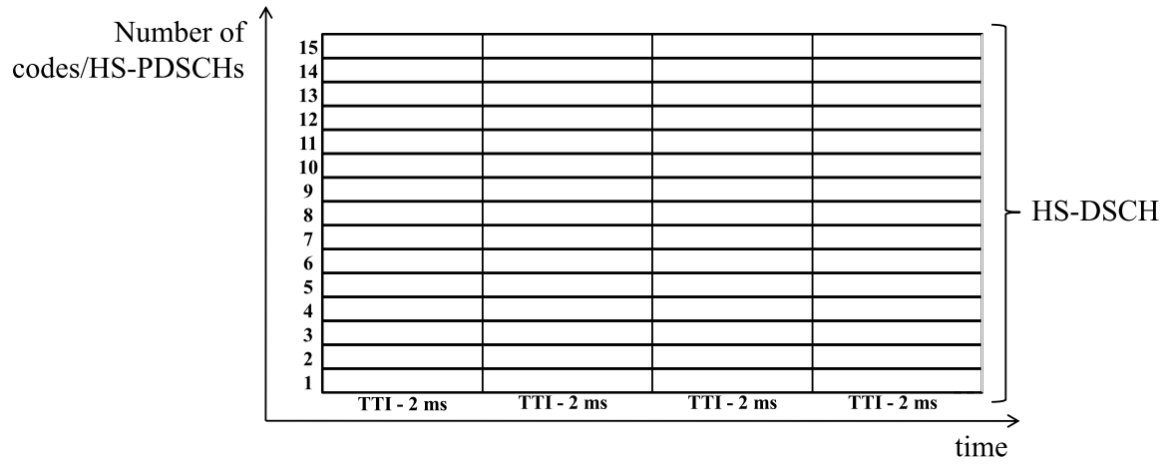

Figure 4.1 *The HS-DSCH can be scheduled in time and in code domain.*

4.2.3 The downlink dedicated channels DPCH and F-DPCH

Although in HSDPA there is not fast-power control in the DL, there is in the UL. Therefore, a downlink dedicated channel is needed so that the Node B can send power control commands to the UE. This channel is called as Downlink Dedicated Physical Channel (DPCH).

In Release 6, support for fractional DPCH, F-DPCH, is added. It seems a waste of resources to use a dedicated channel of SF 256 per user [26], and the F-DPCH resolves this by allowing multiple users to share a single channelization code.

4.3 NodeB-based features

4.3.1 Link adaptation and adaptive modulation and coding

Link adaptation (LA) has been historically deployed in WCDMA networks by means of power control mechanisms. In the case of HSDPA, this is replaced by adaptive modulation and coding (AMC) or rate control [13, 25]. Modulation and coding schemes of the dedicated data channels are changed dynamically depending on the channel conditions. If those are good, allowable data rates can be higher, so higher-order modulations, more number of codes and larger transport block sizes can be used. Link adaptation is performed every TTI at the same time as the scheduling tasks (Section 4.3.3).

4.3.2 HARQ

Fast *hybrid ARQ (HARQ) with soft combining* allows the terminal to request transmissions of transport blocks that have been received erroneously. As mentioned

before, after each received transport block, an ACK or NAK in send back to the Node B and this is done 5 ms after the reception. *Soft combining* means that, in the case the receiver could not decode a receiver transport block, it does not discard it like in traditional HARQ, but keeps it and combines it with subsequent transmissions increasing in this way the probability of successful decoding [13].

The HARQ task is carried out by the MAC-hs sublayer at the Node B. Hence, retransmissions in HSDPA systems are considerably faster than in Release 99 networks whose retransmissions were RNC-based.

4.3.3 Scheduling

In each TTI, the scheduler decides to which user/s and at which rate the shared-channel transmission (HS-DSCH) has to be assigned. In HSDPA, the scheduler entity is channel-dependent. It means that users are scheduled depending on their particular radio-link conditions. This leads to a better performance of the scheduling called *multi-user diversity* [26]. Although the scheduler is not specified by 3GPP, normally it does not take into account only channel conditions but also traffic behavior. In this way, users' activity and service priorities are considered.

The channel-dependent scheduler chooses a predefined TBS and a number of channelization codes depending on the CQI value reported by the UE on the uplink HS-DPCCH. This is why the HS-DSCH is considered as *rate-controlled*. The CQI is a 5-bit number that is calculated at the UE based on the channel conditions. Nevertheless, the CQI value does not just correspond to the E_c/N_0 or SIR of the CPICH, but is the function of more variables, such us intercell interference or terminal type [15]. Furthermore, the way of calculating the CQI is vendor-specific. The CQI is more a "recommended-TBS indicator" than a quality indicator: some terminals are more capable than others of accepting higher data rates and multiple codes. Being the channel conditions the same for two terminals, the terminal with more advanced receiver will be scheduled a higher TBS than the other with simpler receiver (Section 4.4.5). The match between terminal's category, CQI, TBS, number of HS-PDSCHs and modulation, is standardized by the 3GPP in the form of tables that both the Node B and the UE have [27].

4.3.4 Round-trip time

It has been demonstrated that thanks to the reduced TTI of 2 ms in HSDPA, the round-trip time (RTT) is considerably shortened. The RTT in a WCDMA Release 99 channel is between 100 and 200 ms while in HSDPA is normally below 70 ms [25].

4.4 Other general HSPA new characteristics

4.4.1 Mobility and handovers

Mobility in HSDPA refers mainly to the change of *serving* cell [13]. Measurements are reported from the UE to the RNC, which commands the serving cell change based on the measurements. The necessary reconfigurations of the UE and Node Bs can be either synchronous or asynchronous. Asynchronous reconfiguration may imply some data loss [13], so synchronous reconfiguration is more likely to be used. Regardless of the type of reconfiguration, when the UE moves from one Node B to another, the HARQ buffers of the MAC-hs sublayer are not kept and thus, packet losses occur. This situation is handled by the RNC.

4.4.2 MIMO and new modulation schemes

The aim of the introduction of Multiple Input Multiple Output (MIMO) in Release 7 and higher-order modulation schemes in Releases 5 and 7 is to push up the data rates.

MIMO is a technique that, by means of multiple antennas, generate multiple data streams that are mutually orthogonal. In this way, signal-to-noise ratio (SNR) is increased and consequently, capacity is improved. In HSPA+, the MIMO concept developed is the Dual Transmit Adaptive Array (D-TxAA). It has two modes: in a dual-stream transmission, two data streams are encoded and transmitted separately though sharing the same spreading code; in a single-stream transmission, there is only one data stream transmitted by the two antennas [25].

Regarding the modulation upgrades, higher-order modulations mean more bits per symbol, which gives higher data rates. HSDPA (Release 5) introduces the utilization of 16 QAM in addition to the existent QPSK. Release 7 adds 64 QAM to the downlink: higher-order modulation is specially useful when the UE or the Node B are not MIMO-equipped. Actually, the combination of MIMO and 64 QAM would give a theoretical data rate beyond 40 Mbps, but that combination is not included in Release 7. Theoretical peak data rates of WCDMA Release 99, HSPA and HSPA+ are shown in 4.2.

4.4.3 Layer 2 optimization

Release 7 (HSPA+) introduces enhancements to the RLC and high-speed MAC (MAC-hs) protocols. With HSPA, the RLC PDU size is semi-statically configured, feature that is beneficial for low and medium data rates but not for high data rates [13]. The solution that HSPA+ gives is to develop the term *flexible* RLC. This consists on a segmentation of the RLC PDUs into smaller MAC PDUs in the

Table 4.2 *Theoretical downlink data rates of UMTS air interface [25].*

WCDMA specification	Peak DL data rate with approximate 1/1 coding rate
Release 99	384 kbps
Release 5/6	14.0 Mbps
Release 7	28.0 Mbps

Node B. The sizes selected for the MAC PDUs are dependent on the instantaneous radio conditions.

Another issue of the layer 2 optimization is that, with HSPA+ data from different radio bearers can be multiplexed into the same transport block.

4.4.4 Continuous packet connectivity

Continuous packet connectivity is a new feature introduced in HSPA+ Release 7. It resolves the problem of how to manage bursty packet traffic in a more power-efficient way. Packet-data traffic is often bursty with periods of inactivity. From a delay perspective, it is more beneficial to keep on the connection with dedicated downlink and uplink channels. However, this has a cost in terms of terminal's power consumption and uplink interference. A set of three features, known as continuous packet connectivity, addresses that trade-off [13]:

- *Discontinuous transmission (DTX).* In the uplink of HSPA, the presence of the DPCCH causes interference. Switching off this channel completely during inactivity periods would impair UL synchronization and power control mechanisms. The solution that HSPA+ introduces is that, when there is not transmission of the UL dedicated channel, only periodic bursts of the DPCCH are allowed.

- *Discontinuous reception (DRX).* In HSDPA, the UE needs to monitor up to four HS-SCCHs per subframe. In HSPA+, the UE is not required to decode the four shared channels if it is not using the HS-DSCH. Instead, the network restricts the subframes where the UE is allowed to monitor the HS-SCCHs, and this is done in a periodic manner. To fully benefit from DRX advantages, this has to be used always in combination with DTX.

- *HS-SCCH-less operation.* The presence of the HS-SCCH can be seen as a signalling overhead for the network. This overhead is specially noticeable with services as VoIP that typically transmit small payloads. Release 7 introduces

the *HS-SCCH less operation* that consists on allowing the transmission of HS-DSCH without any accompanying HS-SCCH.

4.4.5 UE capabilities

The ultimate condition for achieving the theoretical data rates given before is the UE capabilities. There are 18 categories of HSPA+ terminals [28]. They differ in the following aspects [29]:

- Set of modulations supported: QPSK, QPSK and 16QAM, or QPSK, 16QAM and 64QAM.
- Maximum number of HS-PDSCH that an UE can simultaneously decode.
- Minimum inter-TTI interval that an UE needs between the decoding of a HS-PDSCH and its consecutive.
- Maximum transport block size allowed.
- HARQ buffer size.

5. INDOOR NETWORKS

5.1 Indoor propagation channel

5.1.1 Main characteristics of indoor propagation

In indoors reflecting surfaces causing multipath are very close to the antennas, which means that the deviation of the signal incident angle is high. As a matter of fact, indoor angular spread is considered up to 360º, while macrocellular environment exhibit very low angular spread values (5-10º) [12].

Furthermore, obstacles being close to the antennas leads to small differences in the path length of the original signal and its replicas. Thus, in indoors, the delay spread is considered smaller than 0.01 μs and the coherence bandwidth greater than 16 MHz [12].

Regarding shadowing, its standard deviation is smaller in picocells (Section 5.2.2) than in bigger cells like microcells: the location variability σ_L has been reported to be around 6 dB for the frequency of 1800 MHz.

5.1.2 Main characteristics of the WCDMA radio channel

In indoors the UMTS radio channel is flat-fading while in outdoors is frequency-selective. According to [12], the coherence bandwidth in indoor environment is greater than 16 MHz. WCDMA bandwidth is smaller than this coherence bandwidth and thus, it is considered a narrowband system in indoors. The characteristic small delay spread of indoors makes the utilization of multipath diversity far from useful [6].

5.2 Dedicated indoor networks

5.2.1 Why dedicated indoor networks are needed

In cellular networks, it is estimated that by 2015 the percentage of in-building generated mobile data will be between 80% and 90% [2, 30]. Considering that recent surveys point out that nowadays the percentage of time using mobile internet in indoors is around 50% [3, 30], the issue of the indoor coverage challenge arises. Actually, it is assessed that 45% of households and 30% of businesses experience poor

indoor coverage problem [31].

From a capacity point of view, there is general agreement that the solution to the indoor coverage problem might be based in dedicated indoor systems able to offload the macrocellular network. Some analysts predict that providing indoor coverage by using outdoor macrocells can place up to three times as much strain on the network as the same volume of outdoor traffic [2].

Dedicated indoor networks are also necessary for providing good indoor coverage since building penetration losses attenuate severely the macrocell signal. Eventually, providing indoor service with a macrocell can be used, but this complicates the planning process as the indoor areas behave as a particularity.

To overcome the limitation of outdoor-to-indoor coverage, different solutions have been proposed and implemented. The following sections will cover these approaches.

5.2.2 Picocells

Picocells are cellular low-power base stations installed indoor for providing cellular mobile service. Naturally, they operate on licensed spectrum. They connect to the base station controller of the operator via standard in-building wiring, fiber optic or Ethernet connection [31].

The main advantages of picocells are:

- They are cheaper than standard base stations.
- Their installation costs are relatively low.
- They increase indoor capacity and coverage while offloading the outdoor macro network.

Nevertheless, picocells present one main drawback that is interference. As an example, in buildings close to outdoor cells, a part of the signal coming from outside interferes with the indoor signal [31]. Although increasing the number of picocells per building may increase the system capacity, interference between indoor picocells and between those ones and the outdoor macrocells degrades the overall performance, especially in WCDMA networks.

Picocells are typically deployed in high-dense indoors, like business centers and shopping malls. Also, they can be useful in high-rise buildings where the macrocell signal is particularly weak.

5.2.3 Distributed antenna systems

A distributed antenna system (DAS) aims to provide smooth coverage in indoor by splitting the transmitted power from the base station between several antennas. All

these antennas operate in the same cell and thus are governed by the same parameter settings.

DAS can be connected to repeaters so that the signal coming from outside can be distributed inside the building. Also, they are used for cover long distance environments like tunnels [31]. Depending on the components used, DAS systems can be differentiated in two categories: passive DAS and active DAS. Unlike in active systems, passive systems' components do not need external power supply.

Passive DAS

A passive DAS consist of the following components:

- Coaxial cables, which link the other components of the DAS. They are the big deal in passive DAS because they introduce high loss depending on the distance. Furthermore, the characteristic attenuation increases with the frequency.
- Splitters and tappers, which split the input power into N output signals.
- Attenuators, which low down the signal's power level.
- Filters, which separate frequency bands. The duplexer is used to separate a combined TX/RX signal into separate TX and RX lines. The diplexer an triplexer can separate or combine whole bands like the 2100, 1800 and/or 900 MHz bands.
- Other components like terminators, circulators, etc.

Comparison of active and passive DAS

Traditionally, passive DAS have been used extensively for GSM [19]. Passive systems are straightforward to design, can be installed in harsh environments and their components are manufacturer compatible [19]. However, when facing technologies like UMTS and HSPA new problems arise. Mainly, 3G systems use higher frequencies so they are dramatically affected by attenuation in passive components.

This leads us to the main drawbacks of passive DAS: when the size of the building is considerable, installing coaxial cables is not always possible and balancing the power budget for all antennas is hard. Furthermore, since coaxial cables are hardly bended, their installation is expensive.

On the contrary, active DAS do not report these weaknesses. The ability to compensate for the losses of the cables makes the system very easy and fast to plan [19]. However, active DAS are not suitable for harsh environments like tunnels where active components will easily fail if not shielded.

Taking all of this into account, it can be concluded that passive DAS are more convenient for small buildings while active DAS are for big indoors.

5.2.4 Comparison of DAS and picocells

DAS does not provide any micro diversity, and therefore it does not improve the received E_b/N_0 [6]. Also, if a DAS is dimensioned to cover long indoor distances, it can lead to a situation where the delay spread is high and specially harmful for orthogonality.

Another problem of passive DAS is that part of the signal coming from the base station is attenuated before reaching the antenna end point, so the EIRP per antenna is decreased. Actually, measurements [5,6] have shown that picocells usually provide better RSCP levels.

UMTS picocells have an important drawback that is interference. Most commonly, SIR and E_c/N_0 values are worse than in DAS systems [5, 6]. Although interference decreases the cell capacity, normally system capacity remains better in picocells systems than in DAS due to the higher density of cells.

5.3 Indoor network planning

5.3.1 Planning differences between indoors and outdoors

The scope of indoor planning is to achieve adequate signal quality in the targeted indoor locations. Therefore, indoor planning is a more detailed process. Actually, the placement of the antennas needs to be carefully designed. Most commonly, this is done in a semi-practical manner, meaning that several tests and relocations need to be done after the planning process.

One of the parameters that differ between indoor and outdoor planning is the diversity gain. Most commonly, 3G indoor networks do not use diversity techniques.

5.3.2 WCDMA and HSDPA planning

While in WCDMA networks some cell overlapping is advisable to ensure continuous coverage, in HSDPA networks this is totally unwise. Neither the downlink of HSPA nor the downlink of HSPA+ support soft handover. That means that overlapping cells only cause interference and no gain can be brought out from it.

For HSDPA planning, the Release 99 link budget should always be considered first (Section 3.5) so that the DCH coverage can be determined. Additionally, the HSDPA link budget gives the maximum user throughput achievable at the edge of that coverage [29].

5.3.3 HSDPA indoor link budget

The link budget is the fundamental tool for coverage planning as it gives the maximum allowable path losses in the UL and DL directions. Due to the particularities of HSDPA and indoor networks, a HSDPA indoor link budget presents some differences with regards to what was introduced in section 3.5.

The transmitting end

The EIRP at the transmitting end has to be carefully calculated when facing a DAS transmitter. Losses in coaxial cables and splitters have to be considered. There must be one link budget per antenna in the DAS, as normally EIRP from different antennas is usually different.

The receiving end

What was said for the transmitting end is also applicable for the receiving end if the link budget corresponds to the UL direction.

The parameters of the service profile change when facing HSDPA planning. In HSDPA link budget, E_b/N_0 is not used as performance metrics. Using E_b/N_0 would require to know parameters like the bit rate or this number of codes, which is impossible due to the fact that their values change in every TTI (2 ms). Instead, average SINR allows to create the DL link budget for HSDPA [15].

$$\begin{aligned} SINR &= SF_{16}\frac{P_{HS-DSCH}}{(1-\alpha)\cdot I_{own} + I_{other} + N} \\ &= SF_{16}\frac{P_{HS-DSCH}}{I_{own}}\frac{1}{1-\alpha+G^{-1}}, \end{aligned} \tag{5.1}$$

where SF_{16} is the HS-PDSCH spreading factor of 16, $P_{HS-DSCH}$ is the received power of the HS-DSCH, I_{own} is the received intracell interference, I_{other} is the received intercell interference, N is the noise power and α is the orthogonality factor.

The parameter G is the geometry factor, a key parameter within the performance metrics of HSDPA:

$$G = \frac{I_{own}}{I_{other} + I_{own}}. \tag{5.2}$$

For HSDPA, the receiver sensitivity can be expressed as follows [29, 32]:

$$\begin{aligned} \textit{Receiver sensitivity} &= I_{own} + I_{other} + C/I_{required} \\ &= I_{own} + I_{other} + SINR - PG. \end{aligned} \tag{5.3}$$

The RF channel

In a HSDPA indoor power budget, the margins differ with regard to Release 99 margins [32]:

- there is no soft handover gain;
- the slow fading margin is smaller;
- there is no fast fading margin due to the lack of power control in HSDPA;
- there is no diversity gain.

6. INTRODUCTION TO THE MEASUREMENT CAMPAIGNS

6.1 Overall view

Two measurement campaigns (MCs) were accomplished in Tietotalo building in the months of April, May and June: the Big Room scenario (BR) and the Haroon Shan scenario (HS) MC. I called the first MC as Big Room MC because it took place in a big lecture hall. Then, I gave the name of Haroon Shan MC to the second MC because of the author of the M.Sc. thesis' that accomplished previously in this Department [5], thesis that was taken as reference for the second campaign.

The MCs were held in the context of picocell and DAS indoor networks. The overall scope was to provide practical results about the effect of intercell interference in indoor networks and the side targets were:

- To analyze the effect of intercell interference on modulation and coding in the DL in HSPA indoor networks. For this purpose, single-cell, multiple picocells and DAS arrangements were compared.
- To provide measurement-based conclusions about how throughput (TP) is affected by interference in indoor networks.

Those objectives were accomplished by:

1. verifying and extending some of the measurements carried out by Haroon Shan in his Master's thesis [5];
2. measuring simplified systems in small rooms;
3. testing in open rooms with picocells not separated by walls.

6.2 Nomenclature

The HS measurement campaign was carried out in rooms TC163, TC165 and TC167. Those rooms are re-named as *room B*, *room A* and *room C* respectively. The BR measurement campaign was held in room TB104, one of the lecture halls of Tietotalo building.

Cells with scrambling codes 358, 359, 360, and 361, are normally referred as *cell 358*, *cell 359*, *cell 360* and *cell 361* for simplicity.

There are up to three possible UMTS terminals in the MCs. Always, one of those UEs is carried at walk speed all along the room under test: this handset is called *moving UE*, although the other two handsets are also recording useful data. The moving UE is a category 14 mobile. The two other terminals are a category 14 UE that is named *UE14*, and a category 8 UE named *UE8*.

In a multicell scenario, the situation when all the cells are fully loaded, either by using actual or virtual load (see next section), is called *maximum load (ML)* situation. If the cells are not loaded, and only the moving UE is allowed to perform data transfer, this is called *minimum load (NL)* situation. When there is only one isolated cell, the situation can be called *Single-cell or One-cell*, depending on the MC.

6.3 The concept of virtual load

6.3.1 Definition

Most commonly, when interference-affected scenarios were required to be reproduced, intercell interference was generated by placing multiple UEs performing data transfer in other cells [5]. In this thesis, this procedure is called *actual load*. However, DL interference levels can be high even if the number of users in other cells is low. This happens because the Node Bs always have to transmit the DL common channels [23]. Therefore, an alternative way of causing intercell interference is to manipulate the power allocation settings of the base station so that the power level of the Common Control Channels (CCCH) of the other cells is increased. In this thesis, this methodology is named *virtual load*. Both actual and virtual load techniques are used in the MCs.

Although virtual load methodology is easier to be applied (it requires very few equipments), it introduces the difficulty of how to map the increase of CCCH's power level with the interference level or other-cell load level. For this thesis, I use and extend a fast method for mapping the measured E_c/N_0 at P-CPICH with a level of intercell interference. This was firstly defined by Jarno Niemelä in his PhD's Thesis [33].

6.3.2 Establishing the maximum interference level

On the one hand, an isolated cell can be fully loaded when only one UE is performing data transfer, considering that the UE has the maximum HSDPA category and that there are not core network limitations. On the other hand, given a non-isolated cell,

the maximum intercell interference level that its DL direction could undergo occurs when the surrounding cells have maximum load.

When applying the virtual load methodology, E_c/N_0 is a representative value of the load of the network, because it decreases accordingly with increases in the power level of the common channels:

$$E_c/N_0 = \frac{RSCP}{RSSI} = \frac{P_{P-CPICH}}{P_{P-CPICH} + P_{CCCH}}, \tag{6.1}$$

where $P_{P-CPICH}$ is the power transmitted on the P-CPICH and P_{CCCH} is the sum of the powers transmitted in the rest of channels (AICH, PICH, P-CCPCH and P/S-SCH). Let's call the E_c/N_0 value of a fully-loaded isolated cell as *target* E_c/N_0. It can be stated that, in the non-isolated cell case, the maximum intercell interference is achieved when the surrounding cells have the *target* E_c/N_0. Figure 6.1 clarifies the role of the target E_c/N_0.

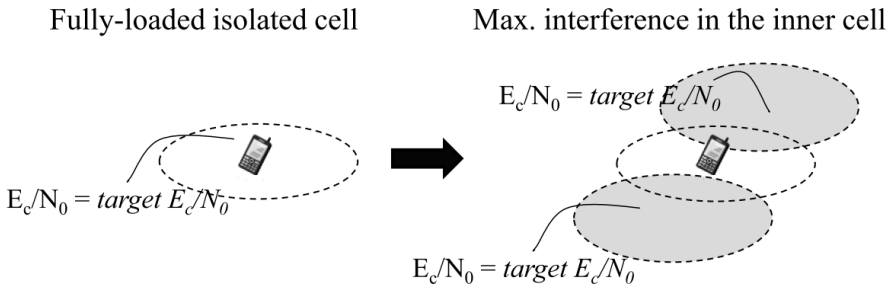

Figure 6.1 *Establishing the maximum intercell interference level by means of* E_c/N_0.

Achieving the *target* E_c/N_0 in a cell can be easily done by increasing the power level of the Primary Common Control Physical Channel (P-CCPCH), i.e., by applying the virtual load methodology.

6.3.3 Establishing different interference level steps

According to [33,34], DL other-to-own cell interference ratio i_{DL} can be derived from E_c/N_0 equation as follows:

$$E_c/N_0 = \frac{RSCP}{RSSI} = \frac{RSCP}{I_{own} + I_{other} + N} = \frac{RSCP/I_{own}}{1 + \frac{I_{other}}{I_{own}} + \frac{N}{I_{own}}} \ . \tag{6.2}$$

By assuming that the contribution of noise can be ignored, we can express i_{DL} [33]:

$$i_{DL} = \frac{RSCP/I_{own}}{E_c/N_0} - 1 = \frac{(E_c/N_0)^{ref}}{(E_c/N_0)^{meas}} - 1, \tag{6.3}$$

where $(E_c/N_0)^{ref}$ is the reference E_c/N_0 and $(E_c/N_0)^{meas}$ is the measured E_c/N_0.

The reference E_c/N_0 is that one that is measured when no intercell interference exists, i.e., when there is only one isolated cell in the scenario. Since E_c/N_0 is affected by TP (sections 3.4.3 and 3.4.4), two different reference E_c/N_0 have to be set, one for measurements in idle mode, and another for measurements in data transfer mode. Figure 6.2 represents the two E_c/N_0 measurements that are needed.

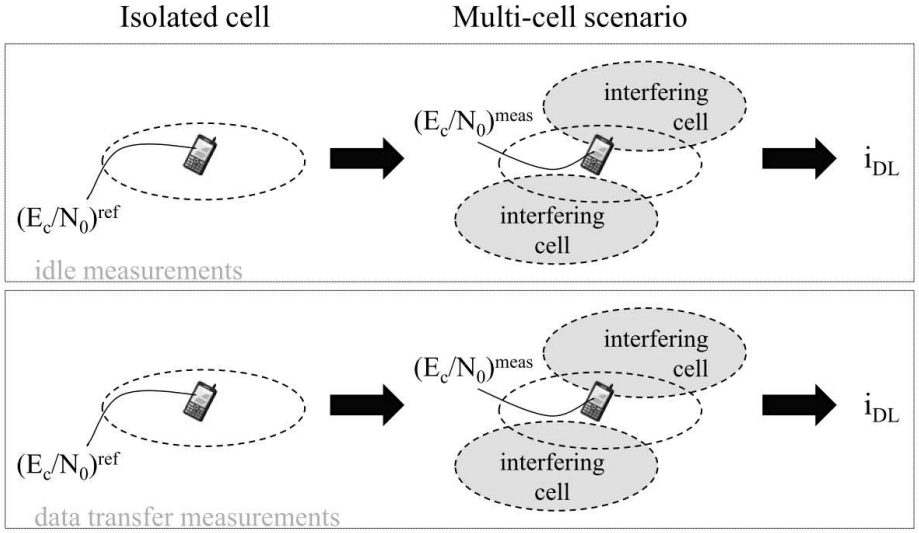

Figure 6.2 *Measurements needed for the mapping between E_c/N_0 and other-to-own cell interference i_{DL} .*

6.3.4 Conclusion

Although the E_c/N_0-to-i mapping methodology may be not very precise [33], and even it could lead to some inconsistences when applying it to data transfer situations, it is a sufficient approach for analyzing the effect of interference in this thesis.

Finally, in the rest of this document, little i can be seen as the intercell interference solely. Note that indoors the orthogonality factor is typically close to 1 and intracell interference can be removed considerably after despreading.

6.4 Measuring equipments

The network under test is a fully functional UMTS Release 7 network. It includes one four-sectored base station connected to a RNC through optic fiber. There are up to three possible measurement equipment sets. All the sets consist of a laptop, an USIM card and the corresponding software. Their main features are summarized in Table 6.1.

Note that the measurements are carried-out under HSPA and not HSPA+. In those tests, 64 QAM was disabled at Node B. More precisely, only the downlink was

subject of study.

Table 6.1 *Measurement equipment used.*

Measurement equipment set	UE's name	UE's category	UE's maximum capabilities	Testing software
set 1	moving UE	cat. 14	15 codes, 64 QAM	Nemo Outdoor v5
set 2	UE14	cat. 14	15 codes, 64 QAM	Nemo Outdoor v5
set 3	UE8	cat. 8	10 codes, 16 QAM	Nemo Outdoor v4

Regarding the handsets, all the measurements were performed by carrying the moving UE at walking speed throughout the room under test. The measuring UE was held at 1 m of distance from the floor. During the data-transfer measurements, the moving UE and *optionally* UE4 and UE14 were downloading a file from a server by means of File Transfer Protocol (FTP). No breaks in transfer occurred.

6.4.1 Parameters analyzed

Some of the parameters analyzed have been already introduced, like RSCP, E_c/N_0 and SIR (Section 3.4), CQI (Section 4.3.3), TBS (Section 3.2.2 and 4.3.3), and little i (Section 6.3.3 and 3.6). Additionally, this Thesis presents results for modulation usage, HS-DSCH usage, system TP, and Shannon system capacity.

Due to link adaptation (Section 4.3.1), modulation changes. Every output sample of the measurement software reports the modulation under use. By means of Matlab post-processing, the number of samples for each modulation are counted and the usage percentage for each modulation (QPSK or 16 QAM) is given.

Every measurement software's sample also contains information about channel usage. The transmission time interval (TTI) is the periodicity at which a TBS is transferred by the physical layer. However, when there are other mobiles in the network there is time scheduling of the HS-DSCH (Section 4.3.3), causing some of the TTI's of the mobile under test remain unused. HS-DSCH usage indicates in percentage how many of the TTI's were used.

System TP refers to the aggregation of the MAC-hs TP of all the mobiles present in the network. MAC-hs TP does not take into account physical layer overhead, but for simplicity, in this Thesis the terms TP and MAC-hs TP are used as synonyms. System TP has been calculated by adding the MAC-hs TP recordings of the moving UE plus the MAC-hs TP of UE14 and UE8 if they are in the scenario. The operation has been made sample by sample; since the rounds differed in the number of samples, some post-processing with Matlab was been needed and fake samples with interpolated values were added to the shortest rounds.

Finally, Shannon system capacity is calculated as follows by taking as reference the measured average SIR:

$$C_{Shannon} = number\ of\ cells \cdot log_2(1 + measured\ SIR). \tag{6.4}$$

6.5 Error analysis

There are three main sources of errors impairing the actual data. Firstly, the software used for recording and processing the measurements of the UEs has a sampling interval of 200 ms. In other words, the UE measurements are averaged over a 200 ms interval. Since the TTI length is 2 ms for HSDPA, the data obtained has a 100 samples precision. This may not affect the average values reported in this Thesis, but most probably affects the results on a time-domain scale: when looking in detail, link adaptation mechanism could appear not to be working properly. The resolution of Nemo Outdoor software must be considered as the most serious source of inaccuracies.

Secondly, the route and way of measuring affects the results. The routes selected covered the whole extension of the room under test. Nevertheless, the measurements with the moving UE were accomplished by carrying the moving UE at walking speed. This means that time and position varied between rounds and velocity could no be maintained perfectly constant. This may have few influence on the overall results, as up to four rounds were accomplished for each measurement case and lately added to conform an average round. The impact of the presence of my body causing Non-Line of Sight situations was tested to be unimportant and more or less constant.

Thirdly, some possibility of error is present in the post-analysis. Graphs and results showed in this Thesis have been generated with Matlab. For an instance, getting the average round vs time graphs required of interpolations. The post-processing must be considered as the less important source of errors.

7. FIRST MEASUREMENT CAMPAIGN: HAROON SHAN SCENARIO

7.1 Introduction: scope of this measurement campaign

Haroon Shan's Thesis was affected by throughput limitations [5]. The first scope of this campaign is to complete the most outstanding measurements of Haroon Shan's but without TP constraints originated at the core network side. In [5,6,35] different indoor solutions namely picocells and DAS were reported to behave differently in terms of signal strength indicators as well as cell and system capacity. The second objective of the HS campaign is to provide practical results about the performance of those indoor networks in high-interference scenarios. The context technology is HSPA Release 6.

7.2 Measurement set-up

7.2.1 Scenario layout

HS scenario was held in rooms A and B 7.1. Rooms' dimensions and measuring route can be found in Figure 7.3. The antennas were omnidirectional of 2 dBi gain [36] and they were placed always at the corners of the rooms. HS scenario hosted three different set-ups:

A) **Two-picocell set-up** (Figure 7.1a). Two cells, one per room, were supported by one single antenna each.

B) **2x2 DAS set-up** (Figure 7.1b). Two cells, one per room, were supported by two antennas each.

C) **Four-picocell set-up** (Figure 7.1c). Four different antennas were located in alternate corners of the rooms. Each antenna corresponded to one different cell.

The moving UE recorded throughout the room following the route in Section 7.2.2. When loaded network wanted to be simulated, load in room B was created with the virtual load methodology. In room A, UE8 and UE14 were the entities in charge of creating the load:

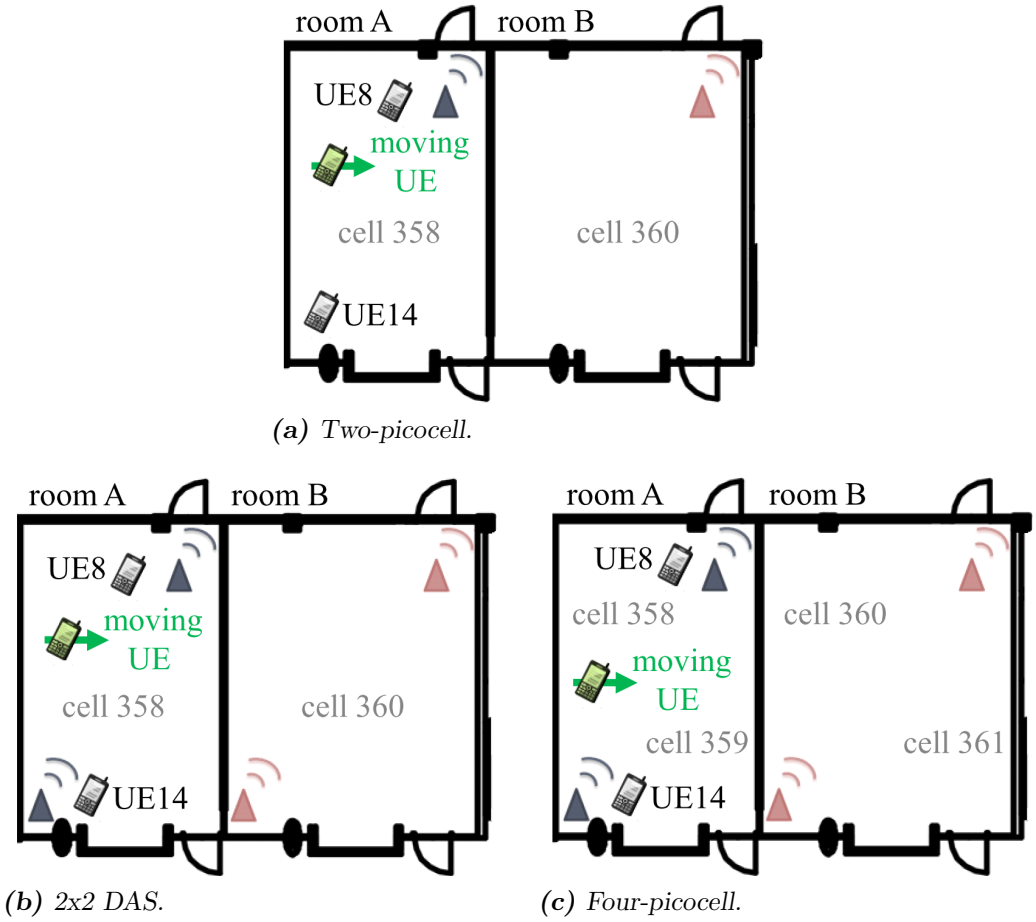

(a) Two-picocell.

(b) 2x2 DAS.

(c) Four-picocell.

Figure 7.1 *Set-ups at HS scenario. Antennas in red correspond to those cells whose power allocation distribution may be affected to support virtual load.*

- UE8 was always attached to cell 358 and situated as in Figure 7.1;
- UE14 was attached to cell 358 in Two-picocell set-up and to cell 359 in the rest of set-ups; it was always situated as in Figure 7.1.

7.2.2 Network configurations and measurement route

Three different network configurations were needed, one per set-up. They are depicted in Figure 7.2. For simplicity, some elements have been omitted: the RNC and Iub interface; the cable between each Node B's cell-plug and the antenna cable; and the connectors.

The measurement route followed with the moving UE had a zig-zag shape (7.3). The aim was to get a fair route, being in the problematic areas (cell re-selection regions and high-interference locations) the same amount of time than in the good areas (Line-of-Sight regions and low-interference locations). UE8 and UE14 remained stationary at the corners of room A.

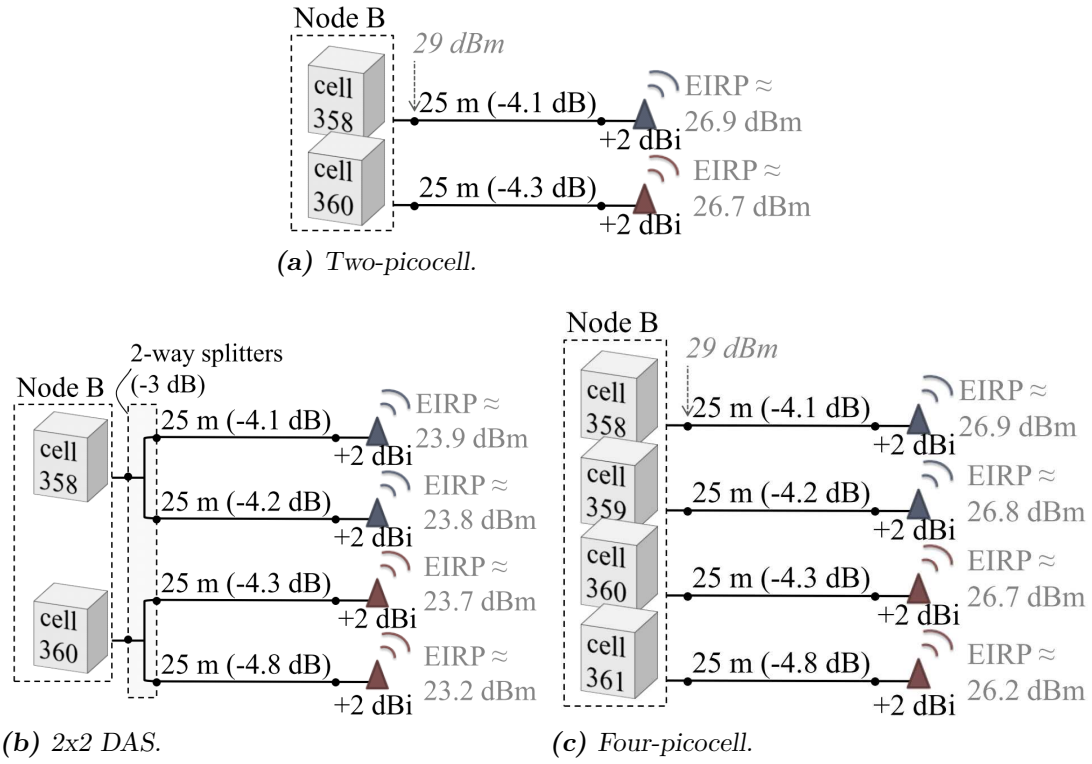

(a) Two-picocell.

(b) 2x2 DAS.

(c) Four-picocell.

Figure 7.2 *Network configurations at HS scenario. Antennas in red correspond to those cells whose power allocation distribution may be affected to support virtual load .*

7.2.3 Measurements performed

Some preliminary measurements were carried out for determining the virtual load level for high-interference situations. They were accomplished with cell 358 in isolated situation, placed at the upper corner of room A. The average E_c/N_0 value measured in data transfer mode was -7.2 dB (Table 7.1). This corresponded with a P-CCPCH power level of +6 dB relative to the pilot channel. Afterwards, this power level would be allocated to cells in room B for generating virtual load.

Table 7.1 *Average E_c/N_0 results with cell 358 in isolated conditions. Preparatory measurements.*

	Idle mode	Data transfer
E_c/N_0	-2.57 dB	-7.20 dB

After the preparatory E_c/N_0 measurements, three sets of measurements were carried out, one per set-up. In NL case, UE8 and UE14 were not present, and cell/s of room B were switched on with normal power allocation distribution. In

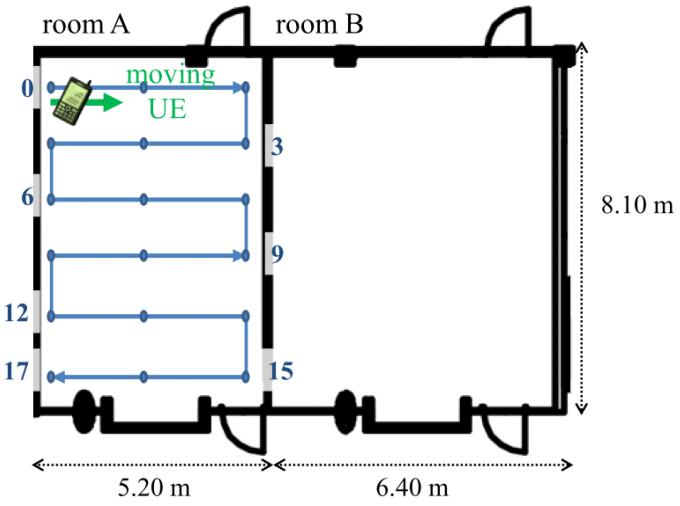

Figure 7.3 *Route followed by the moving UE at HS scenario. Circles represent markers. Markers' numeration begins at 0 and some of them has been pointed out with numbers in the picture.*

ML case, UE8 and UE14 were in the same mode as the moving UE (either idle or data transfer), and cell/s of room B were operational with +6 dB power allocated on P-CCPCH. The measurements are summarized in Table 7.2.

Table 7.2 *Measurements carried-out in HS scenario.*

Set-up	Case	Mode of moving UE
Two-picocell	NL	idle mode
		data transfer
	ML	idle mode
		data transfer
2x2 DAS	NL	idle mode
		data transfer
	ML	idle mode
		data transfer
Four-picocell	NL	idle mode
		data transfer
	ML	idle mode
		data transfer

7.3 Results

7.3.1 Idle mode results

Averaged results for idle mode measurements agree with the expectations (Table 7.3). First, due to the additional loss of splitters, DAS configuration manifests lower RSCP (around 2 dB) than the others. Second, Four-picocell scenario exhibits the lowest E_c/N_0 values. Finally, DAS and Two-picocell configurations behave in the same way in terms of interference. This is logical, as no load is present in room A during idle mode measurements.

Table 7.3 also maps E_c/N_0 values with their respective other-to-own interference factor. As initially forecasted, interference in Four-picocell configuration is higher than in the other two scenarios (little i values exceeding 1).

Table 7.3 *Averaged results from moving UE in room A. Idle mode measurements at HS scenario.*

	Two-picocell		2x2 DAS		Four picocell	
	NL	ML	NL	ML	NL	ML
RSCP (dB)	-33.19	-33.92	-31.76	-31.86	-32.99	-34.22
E_c/N_0 (dBm)	-3.72	-4.38	-3.82	-4.86	-5.81	-6.77
i	0.30	0.52	0.33	0.69	1.11	1.63

Regarding the results obtained by Haroon Shan in his MSc Thesis [5], idle mode RSCP and E_c/N_0 values are a bit higher in the current study. Most probably, this will affect data transfer results being a bit better too than those in Haroon Shan's analysis.

7.3.2 Data transfer mode results

Averaged results for measurements performed in data transfer mode are presented in Table 7.4. Cumulative distribution functions (CDFs) for the principal HSDPA parameters can be found in L2.1 (Appendix B). The data source for the parameters presented is always the moving UE, except for the *system TP*, which is the sum of the MAC-hs TP recordings of the three UEs 6.4.1. Also, calculated Shannon system capacity is shown in Table 8.3 and calculations can be found in Section 6.4.1.

Table 7.4 does not give information about the CQI distribution; this can be found in Figure 7.4. In this last figure, the starting point for 16 QAM utilization has been depicted. This CQI value has been calculated by taking all the configurations' recordings into account (Appendix D). The name "transition region" has been

given to those CQI values that match with 16 QAM utilization around 50 %. The transition region might be caused by inaccuracies in the measurement software.

Table 7.4 *Averaged results from moving UE in room A. Data transfer mode measurements at HS scenario.*

	Two-picocell		2x2 DAS		Four picocell	
	NL	ML	NL	ML	NL	ML
RSCP (dB)	-37.89	-37.68	-35.94	-36.18	-35.76	-37.20
E_c/N_0 (dBm)	-10.55	-12.11	-10.59	-11.84	-8.55	-13.44
little i	1.16	2.10	1.18	1.91	0.36	3.21
SIR (dB)	12.20	11.62	12.52	11.04	9.84	6.67
System TP (Mbps)	9.73	8.57	9.56	9.77	6.09	11.70
TBS (bits)	23101	22319	22817	21638	16457	14646
HS-DSCH usage (%)	99.57	34.48	99.51	36.55	82.13	47.37
Shannon system capacity (Mbps)	31.77	30.38	32.55	29.01	52.40	38.35

On sight of the results, the most outstanding conclusions are:

- **Very small differences between Two-picocell and 2x2 DAS case**. Although DAS could be able to give higher RSCP and E_c/N_0 values, in this case additional losses in the antenna lines compensate that gain. This causes that SIR values are very similar in Two-picocell and DAS cases, and so do it CQI reports (Figure 7.4). In this campaign, the final system TP only slightly higher under the DAS configuration (Table 7.4), but this might be produced by other mechanisms different from link adaptation, like scheduling particularities at the base station. Therefore, when rooms are small and number of cells per room the same, picocells and DAS have similar performance.

- **Four-picocell case is inefficient**. Doubling the number of cells does not double the overall system TP. System TP was calculated as the sum of the MAC-hs TP recordings of the three UEs. In Two-picocell and 2x2 DAS configurations, regardless the serving cell changes performed by the moving UE, the mobiles were always under the same cell (cell 358). In Four-picocell, UE8 and UE14 were in different cells (cell 358 and 359), while the moving UE was passing through different cells. One might expect to have double system TP in the second case, since there were fewer UEs per cell. However, in NL situation, Four-picocell's system TP is 2/3 of the system TP of the other two

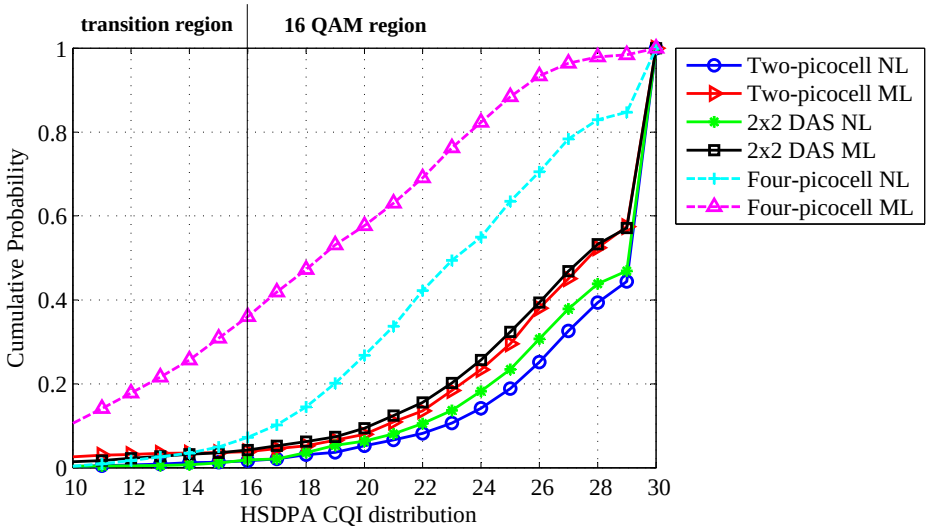

Figure 7.4 *CDFs of CQI values reported by the moving UE at each measurement case. HS scenario.*

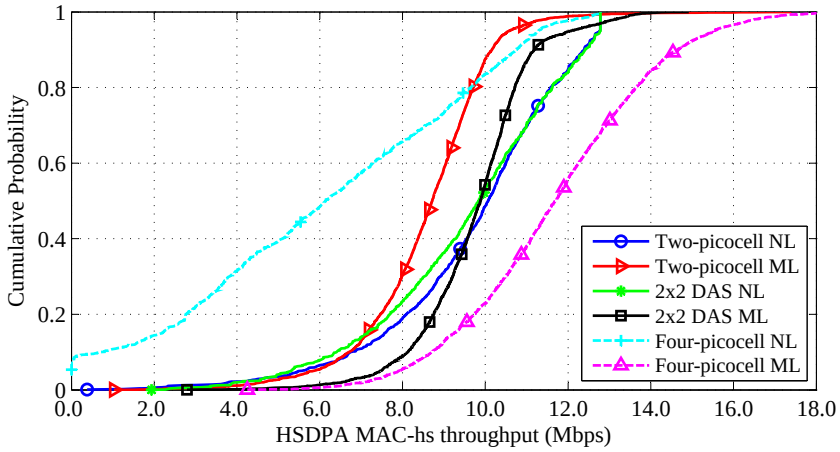

Figure 7.5 *CDFs of system TP at each measurement case. HS scenario.*

configurations. This means that interference is degrading the performance: the 16 QAM utilization percentage drops to 85.5 % (Figure 7.6) and the TBS chosen for the moving UE is much lower too (Figure 7.7).

Similarly in ML situation, Four-picocell's system TP is not the double of the other two set-ups but "only" 2-3 Mbps higher. In conclusion, high-density cell layouts are suitable for small rooms only if the number of users expected in the network is high and there exists a tight demand for capacity. If the number of users or the capacity necessity is forecasted to be low, then low-density cell layouts are the best choice.

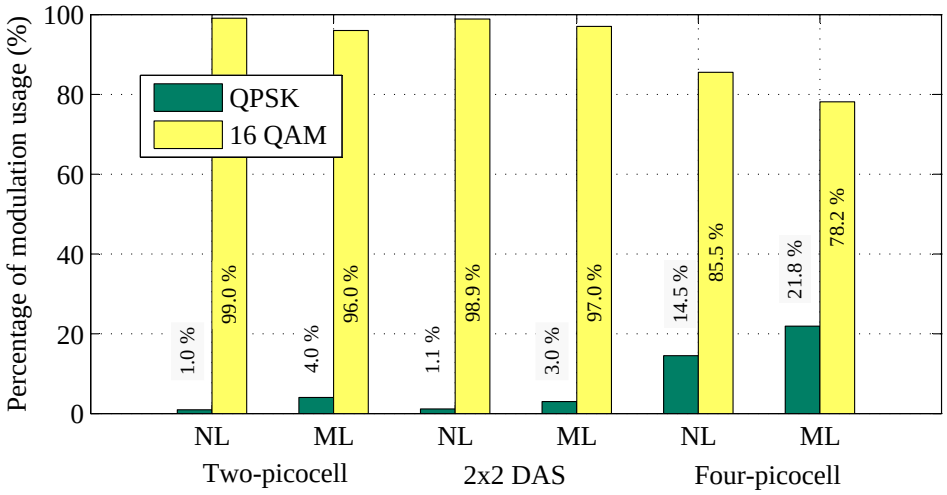

Figure 7.6 *Modulation utilization percentages generated from moving UE recordings. HS scenario.*

- **Increasing number of users change the system TP distribution**. Average system TP values are similar for Two-picocell and 2x2 DAS set-ups, for NL and ML cases. However, increasing the number of users (ML) makes steeper the slope of the system TP CDF: notice the different slope between the green and blue lines (NL), and the red and black lines (ML) in Figure 7.5. This means that in ML cases, most of the samples concentrated around the average instead of usually reporting maximum and minimum TP values.

  The left-most system TP curve belongs to Four-picocell NL case, and the right-most one is the Four-picocell ML case. This means that, although interference affects more the Four-picocell layout as pointed out in the previous point, the presence of more cells enable the system to reach higher data rates. To sum up, high-density cell layouts provide higher system TP, but the maximum system TP achievable is dramatically limited by interference.

- **ML situations are more harmful for the radio-link if the cell density is high**. The degradation of the link quality is bigger in the Four-picocell layout than in the other two configurations. Looking at its ML and NL cases, the distance between their respective CQI CDFs (Figure 7.4) is the biggest (5.5 CQI units), as well as it is the decrease in 16 QAM utilization (7.3 %, Figure 7.6). As a consequence, high load situations need to be considered as one of the key issues when planning an indoor network.

Haroon Shan's Thesis results (Appendix A) were substantially different than those gathered here, due to the constraints coming from the core network [5] and to some

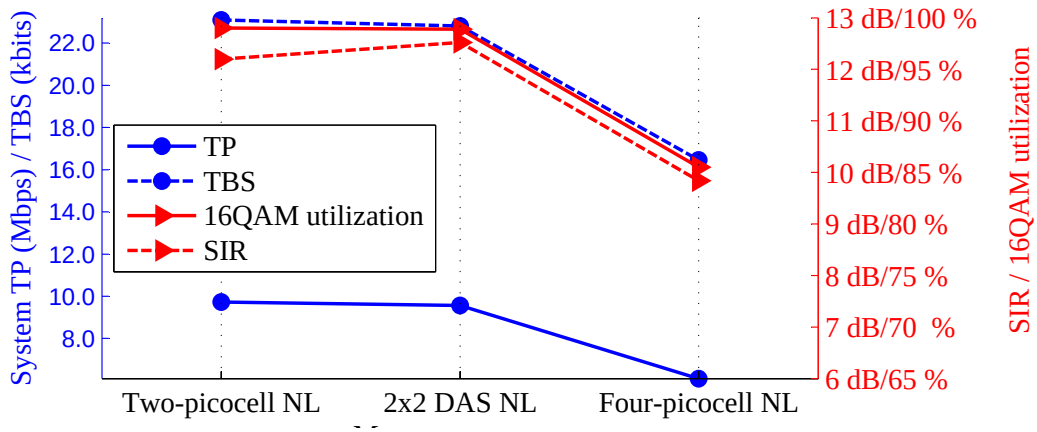

(a) *NL case.*

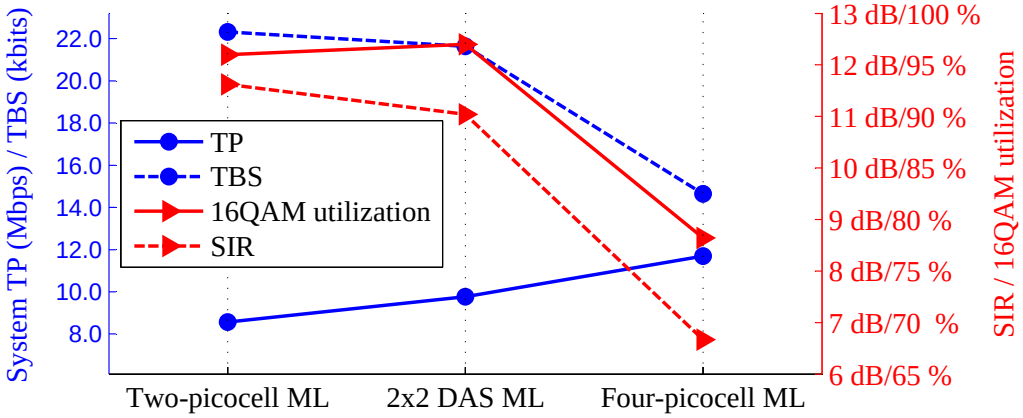

(b) *ML case.*

Figure 7.7 *Dependency between TP, TBS, modulation and SIR at HS scenario.*

changes included in this Thesis' scenario planning. In the Two-picocell case, averaged SIR is similar between the two thesis, but system TP is clearly higher in the current study (8.57 Mbps against 5.10 Mbps). Most probably, this difference is due to the fact that his measurement set-up has a different influence on the recordings (he used two UEs instead of three, the route was planned throughout the high interference areas and there were core network limitations in TP).

Comparison for the 2x2 DAS and Four-picocell case is more fair, as he provided information about the modulation usage. In the case of 2x2 DAS ML, SIR values are similar but QPSK utilization is greatly higher (26.67 %) in Haroon Shan's results than in mine's (3.0 %). Similarly, in the Four-picocell case, even though my averaged SIR is aroun 5 dB worse, QPSK utilization is lower (21.8 % against 35.20 %).

The main conclusions of HS scenario are related to the cell density. When facing small rooms, the isolation of walls is a very handy tool for reducing intercell interference and allowing higher capacity networks. The presence of more than one cell per

room is in general inefficient because interference do not allow to take advantage of the theoretical additional capacity that this would suppose. However, high-density cell layouts should be deployed when a very high number of users with tight capacity demands is expected. Finally, usually only one antenna per room is enough to give good coverage and radio-link quality so the use of two antennas connected to the same cell (DAS) is not necessary.

8. SECOND MEASUREMENT CAMPAIGN: BIG ROOM SCENARIO

8.1 Introduction: scope of this measurement campaign

BR scenario exemplifies the case of open offices. When displaying different picocells, open offices are supposed to undergo with more important interference problems as no walls serve as isolation among cells. Whether it is better to use one single cell or more cells is an issue to be solved. Also, even if the total capacity was better with a multi-cell case, due to interference "bad-capacity" areas would be expected, so that areas should be analyzed as well. In this thesis, related measurement are held in the context of HSDPA Release 6.

8.2 Measurement set-up

8.2.1 Scenario layout

BR scenario was held in rooms TB104. BR scenario hosted three different set-ups:

A) **One-cell set-up** (Figure 8.1a). One cell was supported by a 2 dBi omnidirectional antenna [36] at the middle of the room.

B) **Multicell set-up #1** (Figure 8.1c). Two cells were supported by two antennas each. The antennas were directional of 7 dBi gain [37] and they were placed at the corners of the room. Their main lobes were oriented towards the corners of the room.

C) **Multicell set-up #2** (Figure 8.1b). Two cells were supported by two antennas each. The antennas were directional of 7 dBi gain [37] and they were placed in the center of the room. Their main lobes were oriented towards the corners of the room.

The moving UE recorded throughout the room following the route in Section 8.2.2. When loaded network wanted to be simulated, load was created by UE8 and UE14:

- UE8 was always attached to cell 359 and situated as in Figure 8.1;
- UE14 was always attached to cell 361 and situated as in Figure 7.1.

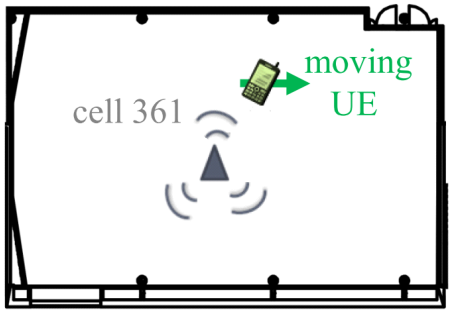

(a) One-cell.

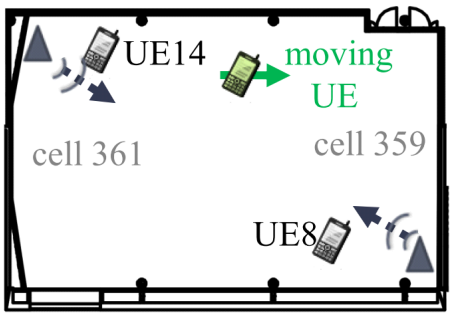

(b) Multicell #1.

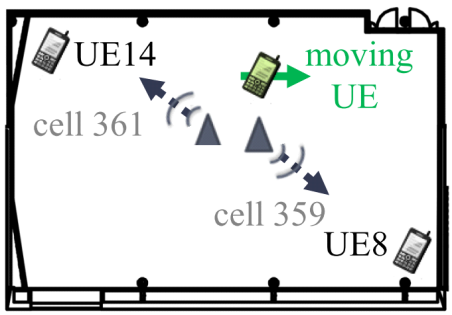

(c) Multicell #2.

Figure 8.1 *Set-ups at BR scenario.*

8.2.2 Network configurations and measurement route

Three different network configurations were needed, one per set-up. They are depicted in Figure 8.2. For simplicity, some elements have been omitted: the RNC and Iub interface; the cable between each Node B's cell-plug and the antenna cable; and the connectors. Finally, the One-cell's antenna line includes a 3 dB attenuator that has been omitted too.

The measurement route followed with the moving UE had a zig-zag shape with a total of thirteen rows separated by 1.5 m distance (see 8.3). The aim was to get a fair route, being in the problematic areas (cell re-selection and high-interference regions) the same amount of time than in the good areas (low-interference locations).UE8 an UE14 remained stationary at the corners of the room.

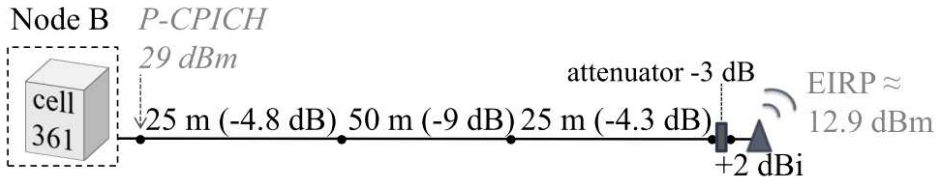

(a) One-cell.

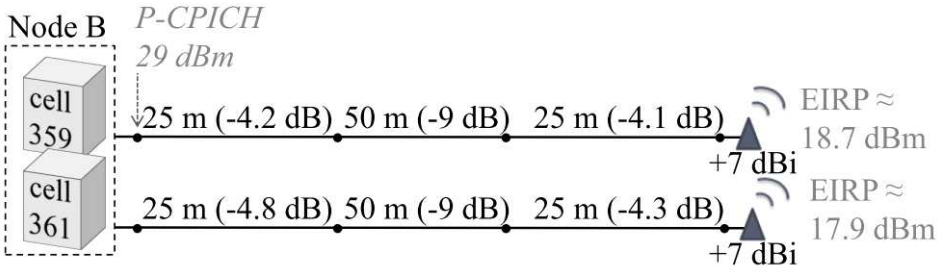

(b) Multicell #1 and #2.

Figure 8.2 *Network configurations at BR scenario.*

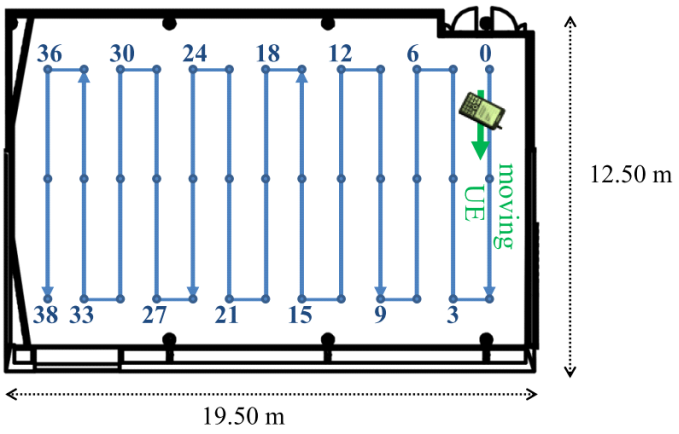

Figure 8.3 *Route followed by the moving UE at BR scenario. Circles represent markers. Markers' numeration begins at 0 and some of them has been pointed out with numbers in the picture.*

8.2.3 Measurements performed

Preparatory measurements were carried out in idle mode. The scope was on the one hand, to get same coverage with cell 359 and cell 361, regardless their location in the room (at the corner or in the centre). In this way, the three configurations could get to be comparable. First, cell 359 was measured, placing the 7 dBi directional antenna in one of the room's corners and using the antenna line of Figure 8.4a ("Cell 359, corner"). Second, the same was done for cell 361 but using the antenna line depicted in Figure 8.4b ("cell 361, corner"). Finally, cell 361 was again measured, but after

changing the directional antenna by the 2 dBi omnidirectional antenna and placing it at the centre of the room (Figure 8.4c, "cell 361, centre, without att"). RSCP CDFs were similar when placing the antennas at the corners but had an offset of +3 dB when a single antenna was situated in the centre of the room (Figure 8.5). For this reason, an attenuator of 3 dB was included in the antenna line of One-cell configuration ("cell 361, centre, with att"). Figure reffig:antlineprep depicts the network configurations of the preparatory measurements explained above, and so matches with the cases presented in Figure reffig:prepcdfs.

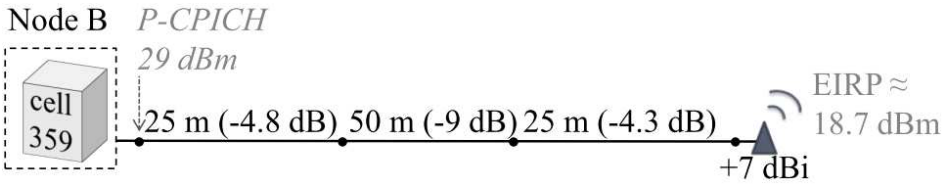

(a) *"Cell 359, corner".*

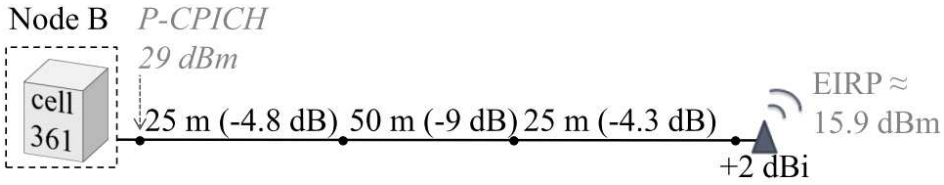

(b) *"Cell 361, corner".*

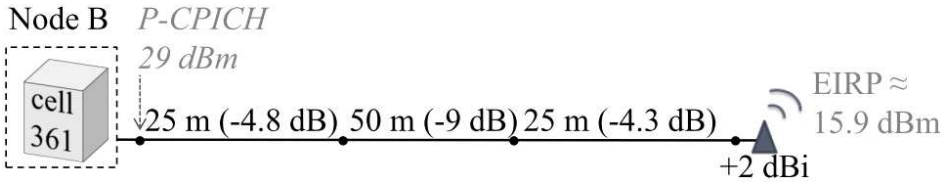

(c) *"Cell 361, centre, without att".*

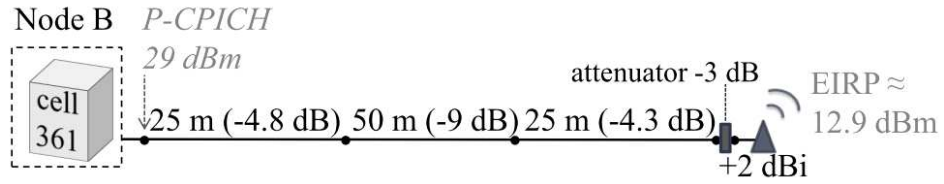

(d) *"Cell 361, centre, with att".*

Figure 8.4 *Network configurations used during the preliminary stage of antenna lines' set-up at BR scenario.*

Three sets of measurements were carried out, one per set-up. In NL case, UE8 and UE14 are not present. In ML case, UE8 and UE14 are in the same mode as the moving UE (that is data transfer). The measurements are summarized in Table 8.1.

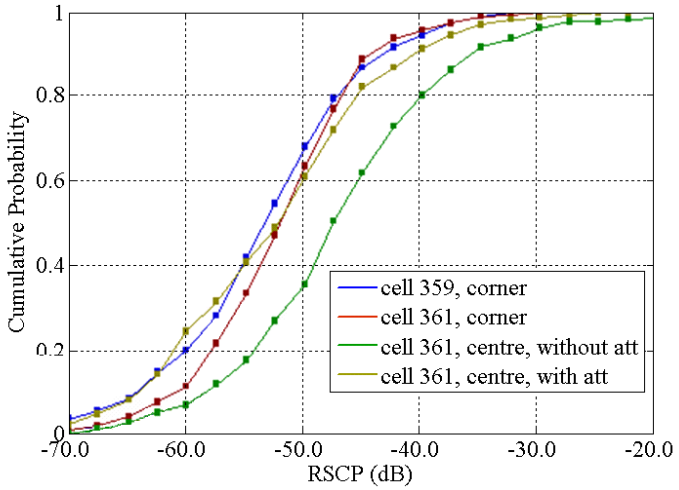

Figure 8.5 *RSCP CDFs generated during the preliminary stage of antenna lines' set-up.*

Table 8.1 *Measurements carried-out in BR scenario.*

Set-up	Case	Mode of moving UE
One-cell	NL	idle mode
		data transfer
Multicell #1	NL	idle mode
		data transfer
	ML	data transfer
Multicell #2	NL	idle mode
		data transfer
	ML	data transfer

8.3 Results

8.3.1 Idle mode results

Averaged results for idle mode measurements are presented in Table 8.2. Surprisingly, the best average RSCP is achieved in Multicell set-up #2 and not in the #1. However, interference has a big impact even if the network has no load: although One-cell's RSCP is around 8.2 dB lower than Multicell #2, its E_c/N_0 is the best one. CDFs of those parameters can be found in Figure L2.2 (Appendix B).

Table 8.2 *Averaged results from moving UE in BR scenario. Idle mode measurements.*

	One-cell	Multicell #1	Multicell #2
	-	NL	NL
RSCP (dB)	-49.99	-47.95	-41.80
E_c/N_0 (dBm)	-2.58	-4.73	-3.59

8.3.2 Data transfer mode results

Averaged results for measurements performed in data transfer mode are presented in Table 8.3. CDFs for the principal HSDPA parameters can be found in L2.2 (Appendix B). The data source for the parameters presented is always the moving UE, except for the *system TP*, which is the sum of the MAC-hs TP recordings of the three UEs 6.4.1. Also, calculated Shannon system capacity is shown in Table 8.3 and calculations can be found in Section 6.4.1.

Table 8.3 does not give information about the CQI distribution; this can be found in Figure 8.6. In this last figure, the starting point for 16 QAM utilization has been depicted. This CQI value has been calculated by taking all the configurations' recordings into account (Appendix D). The name "transition region" has been given to those CQI values that match with 16 QAM utilization around 50 %. The transition region might be caused by inaccuracies in the measurement software.

Table 8.3 *Averaged results from moving UE in BR scenario. Data transfer mode measurements.*

	One-cell	Multicell #1		Multicell #2	
	NL	NL	ML	NL	ML
RSCP (dB)	-50.40	-50.41	-48.61	-44.36	-44.41
E_c/N_0 (dBm)	-7.62	-8.61	-11.95	-9.77	-12.52
SIR (dB)	19.16	11.70	9.21	15.09	12.71
System TP (Mbps)	12.24	8.33	12.55	10.02	12.79
TBS (bits)	25568	21567	18944	23677	22633
HS-DSCH usage (%)	99.92	90.80	47.44	95.47	51.55
Shannon system capacity (Mbps)	24.51	30.57	24.75	38.84	33.00

On sight of the results, the main conclusions derived are:

- **There are not significant changes in modulation usage**. As seen in Figure 8.6, the majority of the CQIs reported are bigger than 26; this short CQI dynamics does not cause almost any change in the 16 QAM usage that is always above 98 % (Figure 8.7). However, TBS and thus coding rate vary considerably: there is a TBS difference of 6624 bits between the highest SIR configuration (One-cell) and the lowest SIR configuration (Multicel #1 ML).

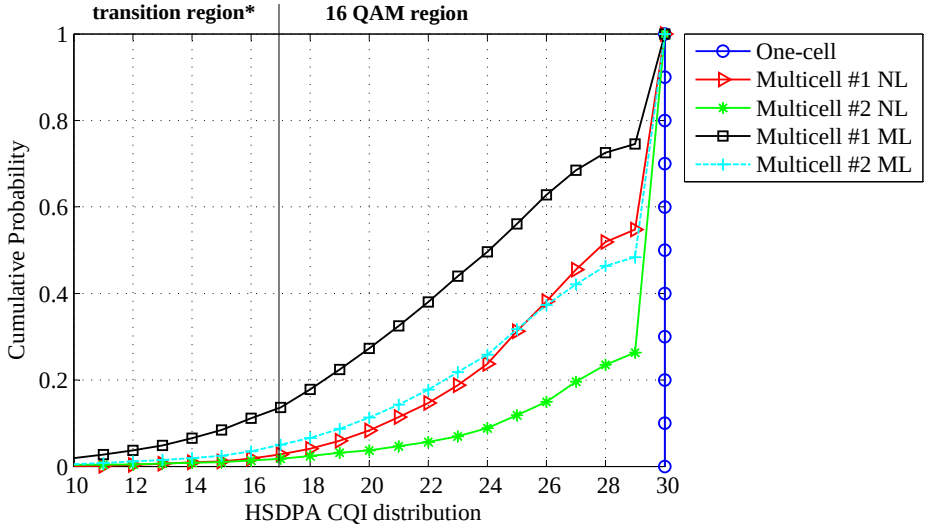

Figure 8.6 *CDFs of CQI values reported by the moving UE at each measurement case. BR scenario.*

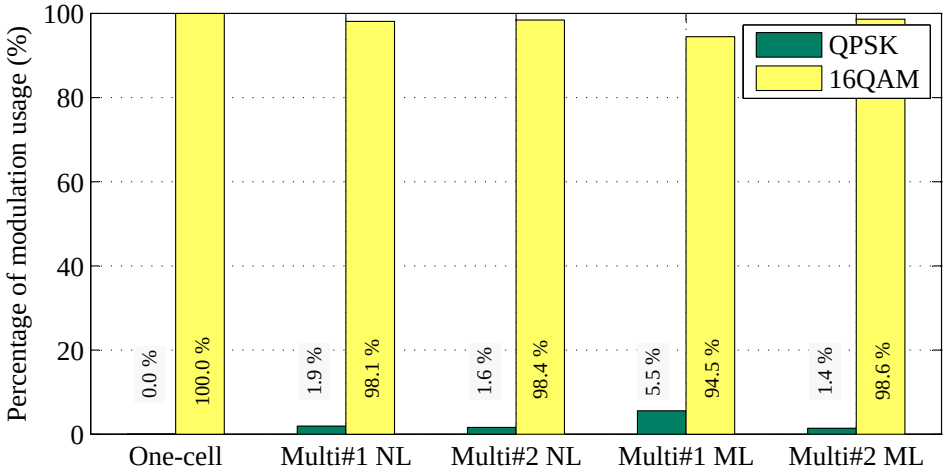

Figure 8.7 *Modulation utilization percentages generated from moving UE recordings. BR scenario.*

- **NL data results are in the line of idle mode results**. Idle mode measurements forecast that Multicell set-up #2 would be the best among the two multicell configurations and also that One-cell set-up, even with lower average RSCP, would be superior in performance to the others. Averaged data transfer results fit with that initial guessing when only one mobile is present in the network (NL).

- **Load levels have an important impact on system TP**. If we had to rank the three configurations according to the calculated Shannon system capacity 8.3, Multicell #2 would be the first, Multicell #1 the second and One-cell the last. However, in NL cases the highest measured system TP belongs to the One-cell configuration, followed by Multicell #2 and Multicell #1 (in this order); while in ML cases, their average system TP values are similar (all of them between 12 and 13 Mbps). Therefore, load has an impact on practical system TP.

- **Overall performance is better in One-cell configuration in no-loaded case**. One-cell configuration exhibits the highest SIR; actually, when the network is no-loaded (NL), One-cell's SIR is 4 dB higher than Multicell #2's that is 4 dB higher than Multicell #1's. As a consequence, the average TBS and system TP are better in One-cell configuration than in Multicell #2 and #1 (in this order). In conclusion, multicell layouts are not suitable for open areas if very few users are expected.

- **Intercell interference degrades the system TP**. The system TP for one cell being 12.24 Mbps, one could expect to have the double TP (24.48 Mbps) with two cells. This supposition can only become true if the TBS would be the same and HS-DSCH usage would be 100 %. However, in ML situation, system TP in Multicell #1 and Multicell #2 is similar to than in One-cell (Table 8.3). When only one mobile is present in the network (NL case), TBS can be compared between the three set-ups: TBS is lower in Multicell #1 and Multicell #2. In conclusion, intercell interference limits considerably system TP.

- **SIR is not the only parameter affecting the CQI decision**. As can be seen in the colormaps of Figure 8.8, the relation between SIR and CQI reports do not follow the shape of a line with positive slope (higher SIR, higher CQI). In spite of this, a lower average SIR causes a scattering in the CQI samples (Figure 8.8b). The interpretation for this behavior is that CQI values' decision is not only SIR-dependent and is vendor-specific. Most probably, some other parameters like BLER or RSCP are being used by the UE for that purpose.

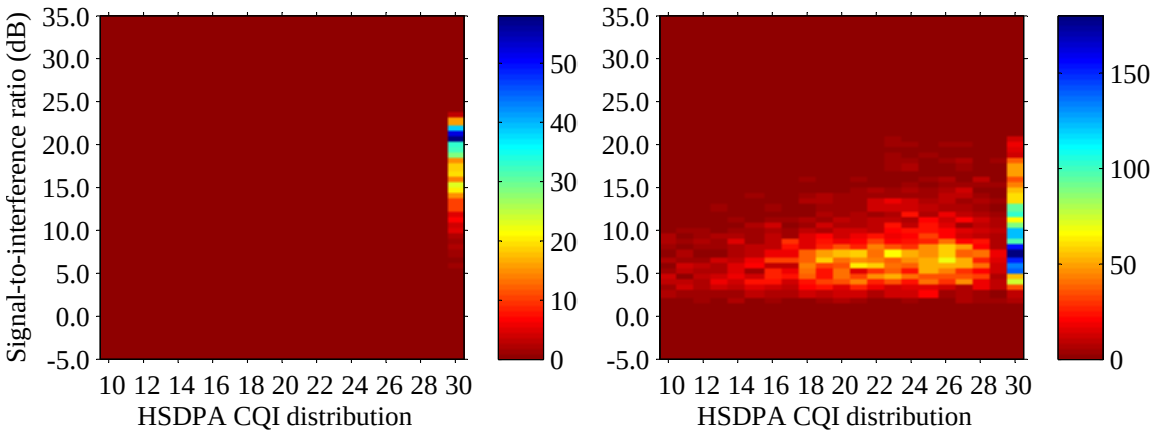

(a) *One-cell.* **(b)** *Multicell #1.*

Figure 8.8 *Connection between SIR and CQI at BR scenario. Number of samples are plotted in a colormap basis.*

Figure 8.9 describes the high interference areas in Multicell #1 and Multicell #2 configurations. More similar figures can be find in Appendix C. In Figure 8.9a, it can be seen that the high-interference region for Multicell #1 is larger (markers 4 to 8, 11 to 28, and 30 to 4) than for Multicell #2, which only have drops in some specific points (markers 4 to 8, 11 to 13, 25 to 27, and 30 to 34). Multicell #1's interference region consists on a wide area centered in the middle of the roon. Multicell #2's interference region appears near the centre of the left and right walls. For this reason, Multicell #2 seems more appropriate than Multicell #1 as users may not usually be situated close to the walls.

Also, in the high-interference areas mentioned above, the user experiences unbearable low data rates. The moving UE gets data rates below 5 Mbps, which would not be a bad value if there were more users in the network, but which is clearly below the maximum 12 Mbps that it achieves sometimes. It is expected then, that the allocated data rate when more users were in the network (ML) would be dramatically low.

Figure 8.9b shows that the One-cell's system TP stays stable as there is no interference and no scheduling. Drops in SIR (Figure 8.9a) coincide with drops in system TP for the other two configurations, so the effect of intercell interference becomes clear. However, looking at the average values of system TP (Table 8.3), Multicell #1 and #2 differ by almost 2 Mbps at NL case, and by only 0.2 Mbps at ML case. This means, that under high-load situations, performance of any multicell layout becomes similar.

Taking all of this into account, it can be concluded that indoor open areas need of a carefully planning that must take into consideration not only the density of cells

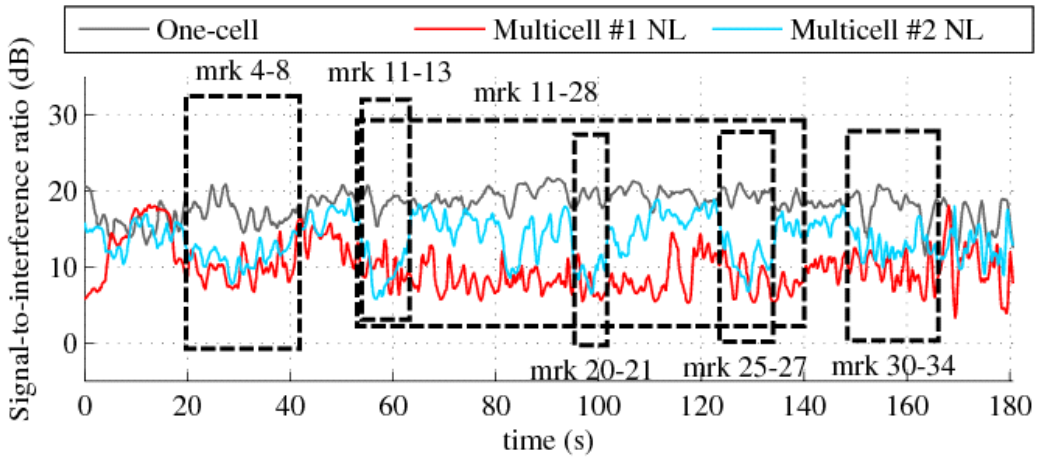

(a) *SIR in NL situations.*

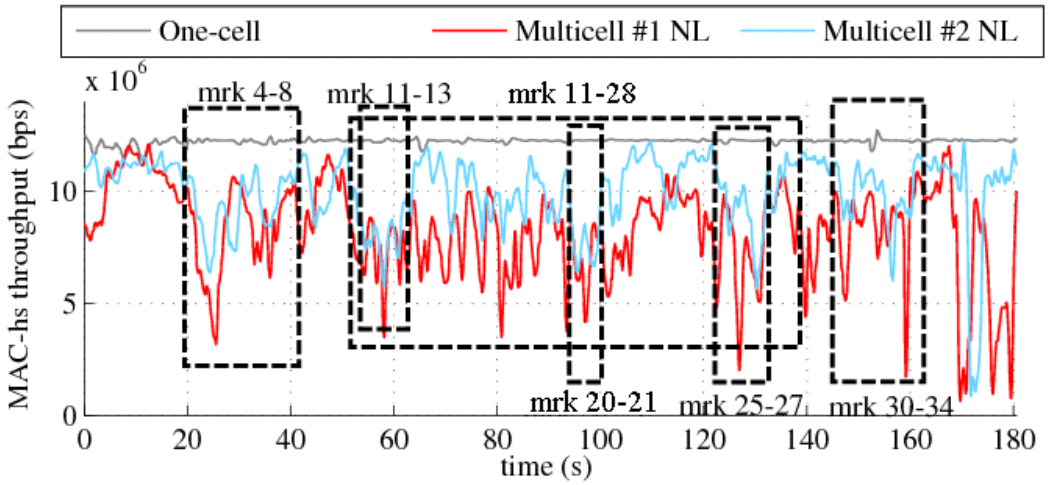

(b) *system TP in NL situations.*

Figure 8.9 *Behavior of SIR and system TP versus time at BR scenario.*

but also the position of the antennas. Overlapping dominance areas cause high-interference regions where capacity is dramatically degraded. Therefore, these areas must be reduced and located in such a way that the most of the users do not feel affected. Whether multicell layouts are better for indoor open areas than single-cell layouts needs still of further study. In this case, it was demonstrated that the gain in system TP of having two cells instead of one was marginal. In conclusion, indoor planning for open areas must consider that the statement "double number of cells implies double capacity" is not always true.

9. CONCLUSIONS AND DISCUSSION

The scope of this Master of Science Thesis was to give practical results regarding the influence of intercell interference on indoor networks as well as guidelines for indoor radio network planning. The context technology for the study was HSPA. WCDMA-based networks are especially affected by interference and the link adaptation mechanism present in the last releases of 3GPP allows a straightforward tracking of the effects of interference. The indoor planning guidelines here presented are classified per type of indoor environment. On the one hand, the Thesis extends the measurements carried out in [5], which enables to reach more fair conclusions for indoor deployment in small room layouts. On the other hand, it presents practical results for an indoor open area and so shows the effect of intercell interference in such areas. As side outcome, the Thesis gives proof of the difficulties of indoor planning, showing that initial suppositions about the performance of the network may be wrong in practice due to the effect of interference.

The extension for the measurements in [5] was accomplished in two small rooms. This environment was called Haroon Shan (HS) scenario. The first main conclusion of this measurement campaign is that performance of picocell and DAS set-ups is similar when rooms are small and number of cells per cell is the same. Proof of that is that their respective calculated other-to-own cell interference i_{DL} was almost coincident and their respective CQI CDFs were overlapping. The second conclusion derived from the HS scenario is that high-density cell layouts are suitable for small rooms only if the number of users expected in the network is high and there exists a tight demand for capacity. However, the interference present in multicell layouts limit considerably the maximum system TP. Walls isolation is the essential key for planning in small-room environments.

The tests over an indoor open area were performed in a lecture hall. This environment was named Big-Room (BR) scenario. The aim of this measurement campaign was to determine the best option for an indoor open area, whether a low-density cell layout (one cell in the room) or a high-density cell layout (two cells in the room). For the two-cells layout, the antennas were located first in the corners pointing to the center of the room, and second in the center pointing to the corners of the room. Surprising results were gathered. For example, there were not big changes in modulation utilization between the three set-ups. However, differences were found in SIR,

TBS and thus system TP. Two-cell layout with antennas in the corners exhibited the lowest average SIR levels and so TBS values, as well as the largest high-interference areas. When antennas were placed in the center, better cell isolation was achieved and interference regions became smaller and moved close to the walls. However, in high-load situations, both two-cell layouts had similar system TP. Regarding the differences between the one-cell and the two-cell configurations, the gain in system TP of adding one more cell was reported to be marginal. In conclusion, there are two considerations to be analyzed when planning a network in an indoor open area: first, multicell layouts are not always advisable to be deployed; second, in case multicell layouts were needed, the impact of antennas' position is particularly significant when load levels are not critical. In multicell configurations, high-interference areas appear so they need to be reduced and placed in such a way that the most of the users do not notice severe TP contraints.

There are some general conclusions that can be derived from this thesis. First, whether if picocells or DAS are better for indoor coverage from an interference perspective depends largely on the type of indoor area (size of the rooms). When both picocells and DAS systems have the same number of cells per room, their performance may be equal. Second, it can happen that multicell layouts do not give the expected higher capacity because of intercell interference. Those two issues must be considered when designing an indoor dedicated network.

BIBLIOGRAPHY

[1] Traffic Management Strategies for Operators. White paper, Qualcomm, January 2011. http://www.cdg.org/resources/files/white_papers/Traffic_Mgmt_and_Offload_White_Paper_Jan2011_v2.pdf.

[2] Matt Hatton and Terry Norman. The message from MWC 2010: indoor coverage and subscriber management are the keys to dealing with exponential growth in wireless traffic. http://www.analysysmason.com/About-Us/News/Insight/The-message-from-MWC-2010/, March 2011.

[3] Cisco visual networking index: Global mobile data traffic forecast update, 2010–2015. White paper, Cisco, February 2011. http://www.cisco.com/en/US/solutions/collateral/ns341/ns525/ns537/ns705/ns827/white_paper_c11-520862.pdf.

[4] GSA. The GSA Mobile Broadband Update: WCDMA-HSPA, HSPA+ and LTE Status Worldwide. Technical report, Global mobile Suppliers Association (GSA), June 2011.

[5] Haroon Shan. *Comparison of picocell and DAS configuration with HSPA evolution.* Master's thesis, March 2011. Tampere University of Technology.

[6] Tero Isotalo, Jukka Lempiäinen, and Jarno Niemelä. Indoor Planning for High Speed Downlink Packet Access in WCDMA Cellular Network. *Wireless Personal Communications*, 52:89–104, January 2010.

[7] M. Yavuz, F. Meshkati, S. Nanda, A. Pokhariyal, N. Johnson, B. Raghothaman, and A. Richardson. Interference management and performance analysis of UMTS/HSPA+ femtocells. *Communications Magazine, IEEE*, 47(9):102 –109, September 2009.

[8] R.E. Schuh and M. Sommer. W-CDMA coverage and capacity analysis for active and passive distributed antenna systems. In *Vehicular Technology Conference, 2002. VTC Spring 2002. IEEE 55th*, volume 1, pages 434 – 438 vol.1, 2002.

[9] R.E. Schuh, R. Andersson, A. Stranne, M. Sommer, and P. Karlsson. Interference analysis for dedicated indoor WCDMA systems. In *Vehicular Technology Conference, 2003. VTC 2003-Fall. 2003 IEEE 58th*, volume 2, pages 992 – 994 Vol.2, oct. 2003.

[10] Simon R. Saunders and Alejandro Aragón Zavala. *Antennas and Propagation for Wireless Communication Systems.* John Wiley & Sons, Ltd, 2nd edition, 2007.

[11] Andrea Goldsmith. *Wireless Communications.* Cambridge University Press, 2005.

[12] Jukka Lempiäinen and Matti Manninen. *UMTS Radio Network Planning, Optimization and QoS Management: For Practical Engineering Tasks.* Kluwer Academic Publishers, 2004.

[13] Erik Dahlman, Stefan Parkvall, Johan Skold, and Per Beming. *3G Evolution: HSPA and LTE for Mobile Broadband.* Academic Press, 1 edition, 2007.

[14] Third Generation Partnership Project (3GPP). http://www.3gpp.org.

[15] Harri Holma and Antti Toskala. *HSDPA/HSUPA for UMTS: High Speed Radio Access for Mobile Communications.* John Wiley & Sons, Ltd, 2006.

[16] Harri Holma and Antti Toskala. *WCDMA for UMTS. Radio Access for Third Generation Mobile Communications.* John Wiley & Sons, Ltd, 3rd edition, 2004.

[17] 3GPP. Physical layer - Measurements (FDD) (Release 1999). TS 25.215, Third Generation Partnership Project (3GPP), March 2005.

[18] Tero Ojanperä and Ramjee Prasad, editors. *Wideband CDMA For Third Generation Mobile Communications: Universal Personal Communications.* Artech House, Inc., 1st edition, 1998.

[19] Morten Tolstrup. *Indoor Radio Planning. A Practical Guide for GSM, DCS,UMTS and HSPA.* John Wiley & Sons, Ltd, 2008.

[20] Chris Braithwaite and Mike Scott. *UMTS Network Planning and Development: Design and Implementation of the 3G CDMA Infrastructure.* Newnes, 2004.

[21] Maciej J. Nawrocki, Mischa Dohler, and A. Hamid Aghvami. *Understanding UMTS Radio Network. Modelling, Planning and Automated Optimisation.* John Wiley & Sons, Ltd, 2006.

[22] Sharad Sambhwani, Wei Zhang, and Wei Zeng. Uplink Interference Cancellation in HSPA: Principles and Practice. Technical report, Qualcomm Inc., January 2009. http://www.qualcomm.com/documents/uplink-interference-cancellation-hspa-principles-and-practice.

[23] Jaana Laiho, Achim Wacker, and Tomás Novosad, editors. *Radio Network Planning and Optimisation for UMTS*. John Wiley & Sons, Ltd, 2nd edition, 2006.

[24] T. Kolding, K. Pedersen, J. Wigard, F. Frederiksen, and P. Mogensen. High Speed Downlink Packet Access: WCDMA evolution. *IEEE Vehicular Technology Society News*, February 2003. http://kom.aau.dk/group/05gr943/literature/hsdpa/evolution%20of%20HSDPA.pdf.

[25] Harri Holma and Antti Toskala. *WCDMA for UMTS. HSPA Evolution and LTE*. John Wiley & Sons, Ltd, 2007.

[26] 3GPP. High Speed Downlink Packet Access (HSDPA); Overall Description; Stage 2. TS 25.308, Third Generation Partnership Project (3GPP).

[27] 3GPP. Physical layer procedures (FDD) (Release 7). TS 25.214, Third Generation Partnership Project (3GPP), March 2003.

[28] 3GPP. User Equipment (UE) radio transmission and reception (FDD) (Release 7). TS 25.101, Third Generation Partnership Project (3GPP), September 2010.

[29] Christophe Chevallier, Christopher Brummer, Andrea Garavaglia, Kevin P. Murray, and Kenneth R. Baker. *WCDMA (UMTS) Deployment Handbook. Planning and Optimization Aspects*. John Wiley & Sons, Ltd, 2006.

[30] Terry Norman. Fixed–mobile substitution: a reversal of fortune for fixed operators. *Mobile insight and the connected consumer. Publication for Mobile World Congress 2011*, 2011. http://www.analysysmason.com/forms/Mobile_World_Congress_2011/Mobile_World_Congress_2011.PDF.

[31] Jie Zhang and Guillaume de la Roche. Indoor Coverage Techniques. In *Femtocells: Technologies and deployment*, pages 15–38. John Wiley & Sons, Ltd, 2010.

[32] Tero Isotalo, Panu Lähdekorpi, and Jukka Lempiäinen. *HSDPA/HSUPA handbook*, chapter 12. CRC Press, 2011.

[33] Jarno Niemelä. *Aspects of Radio Network Topology Planning in Cellular WCDMA*. PhD thesis, September 2006. Tampere University of Technology.

[34] Jarno Niemelä, Jakub Borkowski, and Jukka Lempiäinen. Using Idle Mode E_c/N_0 Measurements for Network Plan Verification. In *8th IEEE International Symposium on Wireless Personal Multimedia Communications (WPMC'05)*.

[35] Tero Isotalo, Panu Lähdekorpi, and Jukka Lempiäinen. Improving HSDPA Indoor Coverage and Throughput by Repeater and Dedicated Indoor System. *EURASIP Journal on Wireless Communications and Networking*, 2008:11, 2008. http://www.hindawi.com/journals/wcn/2008/951481/abs/.

[36] Kathrein. Kathrein 741 573 VPol Indoor 1710-2700 360° 2dBi.

[37] Kathrein. Kathrein 800 10248 VPol Indoor 806-960/1710-2500 90° 7dBi.

APPENDIX A

Table L1.1 *Haroon Shan's Thesis measurement results used for comparison. The case "Two picocells" is the "Two picocells in different rooms" layout that belongs to the "Two antennas scenario" and the cases "Four picocells" and "2x2 DAS" belong to the "Four antennas scenario, configuration 2" [5].*

	Two picocells		Four picocells	2x2 DAS
	Low load	High load	High load	High load
RSCP (dBm)	-38.54	-37.76	-33.57	-38.56
E_c/N_0 (dB)	-7.39	-7.85	-6.97	-7.27
SIR (dB)	12.12	11.69	9.87	11.27
Cell TP (Mbps)	3	2.55	1.4	3.58
System TP (Mbps)	6	5.1	5.61	7.16
QPSK utilization (%)	-	-	35.2	26.67
16 QAM utilization (%)	-	-	50.82	34.88
64 QAM utilization (%)	-	-	13.98	38.46
Shannon system capacity (Mbps)	31.58	30.55	52.53	29.55

APPENDIX B

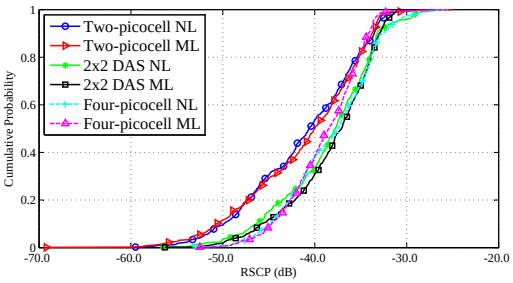

(a) RSCP.

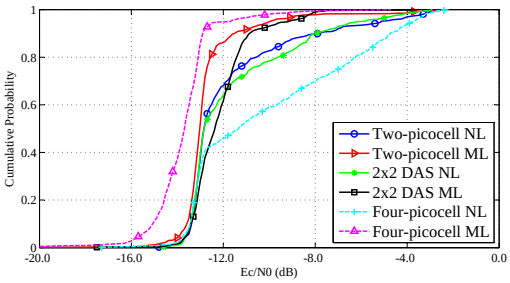

(b) E_c/N_0.

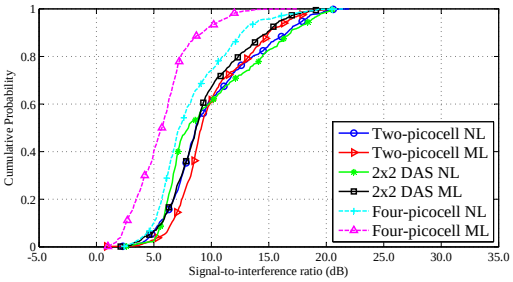

(c) SIR.

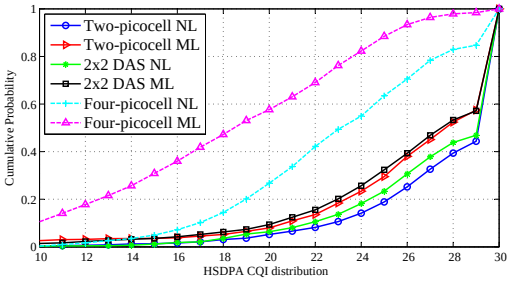

(d) CQI.

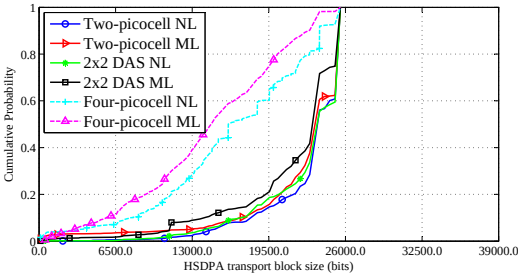

(e) TBS.

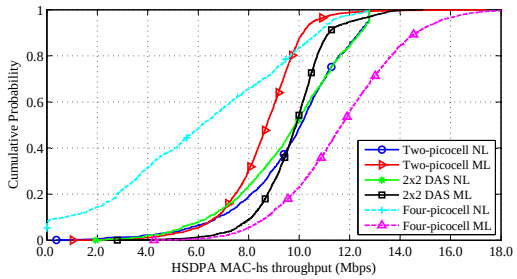

(f) System TP.

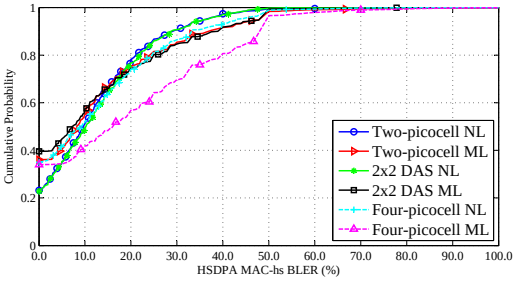

(g) BLER.

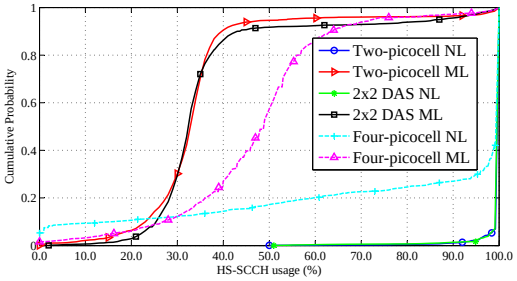

(h) HS-DSCH usage.

Figure L2.1 *Impact of intercell interference and load in HS scenario. Main parameters' CDFs for each of the data transfer measurement cases.*

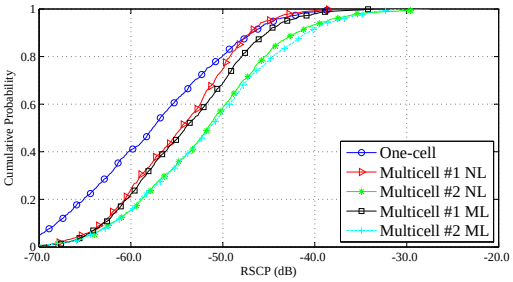

(a) RSCP.

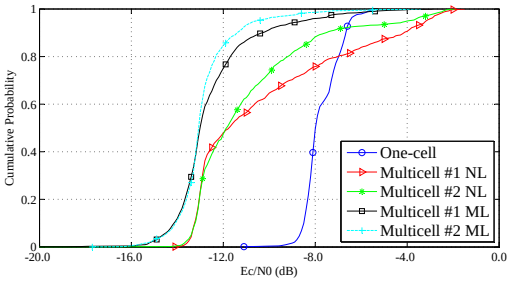

(b) E_c/N_0.

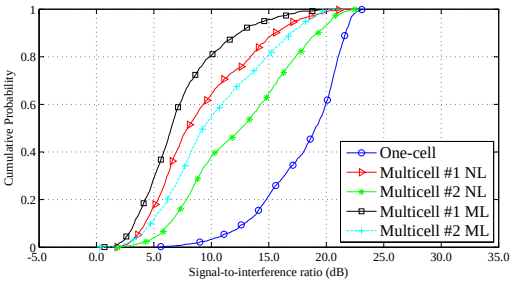

(c) SIR.

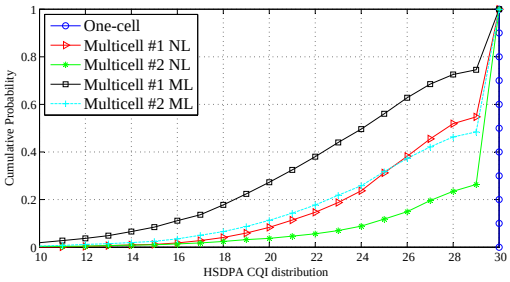

(d) CQI.

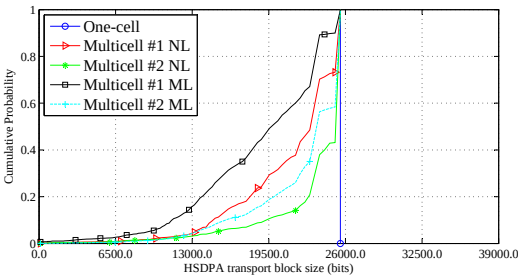

(e) TBS.

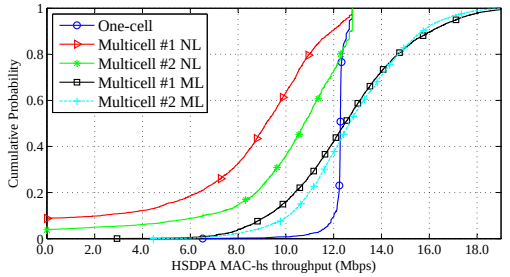

(f) System TP.

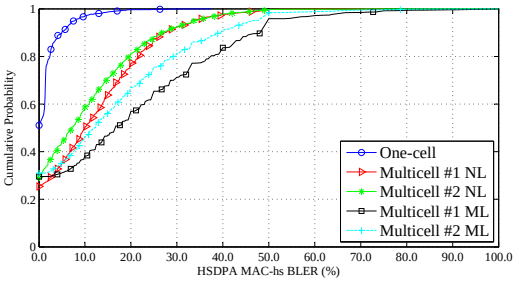

(g) BLER.

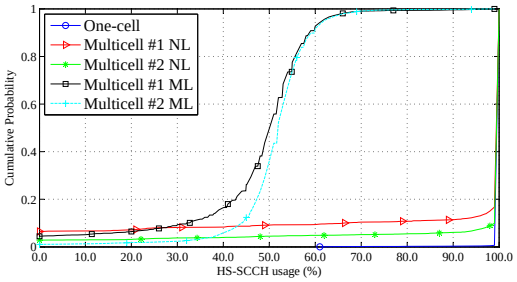

(h) HS-DSCH usage.

Figure L2.2 *Impact of intercell interference and load in BR scenario. Main parameters' CDFs for each of the data transfer measurement cases.*

APPENDIX C

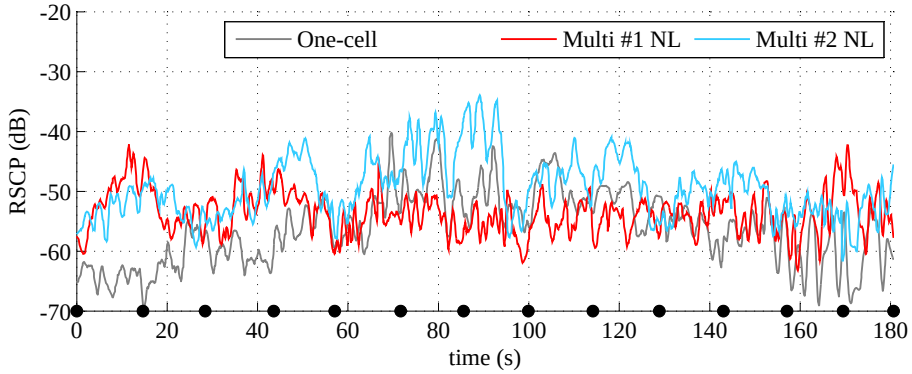

(a) RSCP.

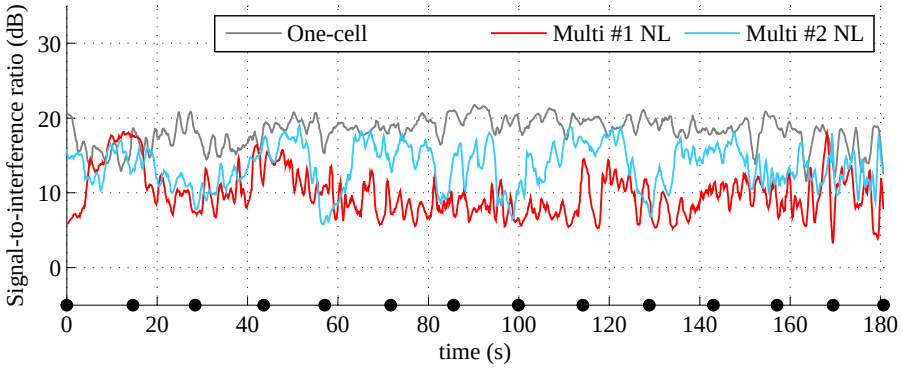

(b) SIR.

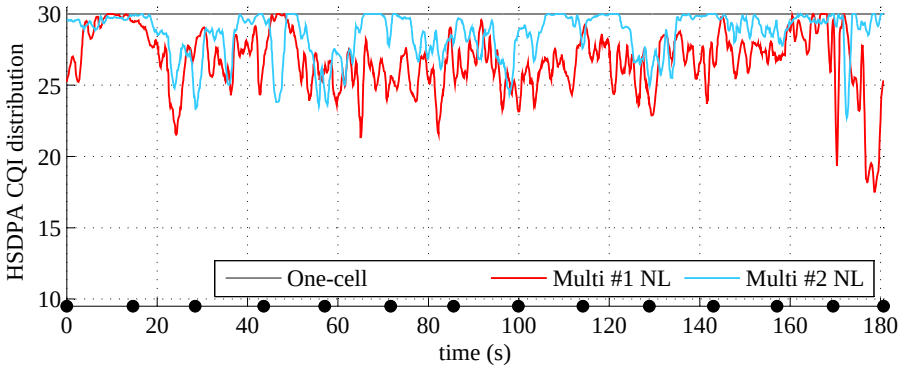

(c) CQI.

Figure L3.1 *Behavior of RSCP, SIR and CQI versus time in BR scenario under NL situation. Graphs have been smoothed in Matlab by means of a moving average of resolution 17. Lines plotted are the result of the combination of the four rounds performed for each measurement case. The points that appear at the bottom of the graph indicate the beginning of each route's row, i.e., markers 0, 3, 6, 9 and so on.*

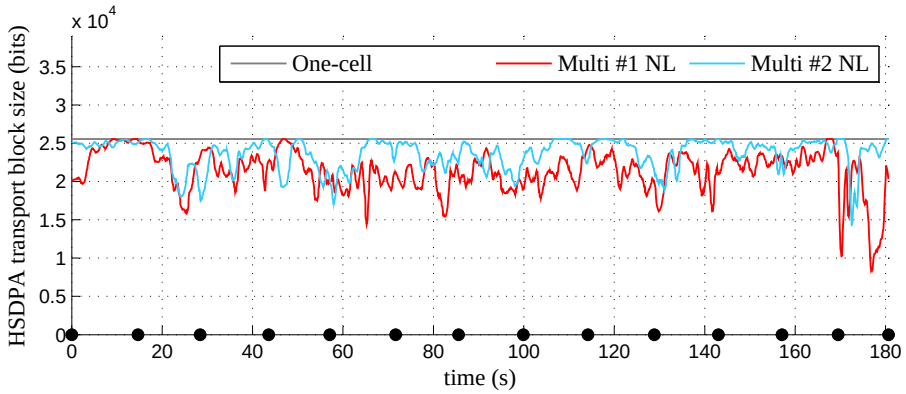

(a) TBS.

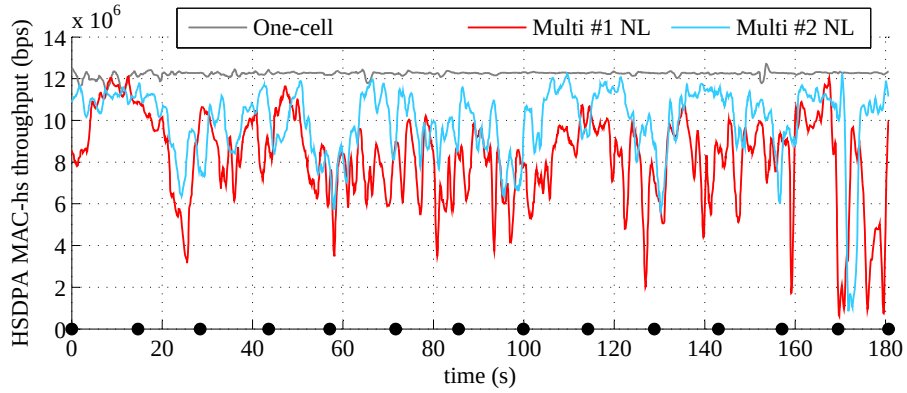

(b) System TP.

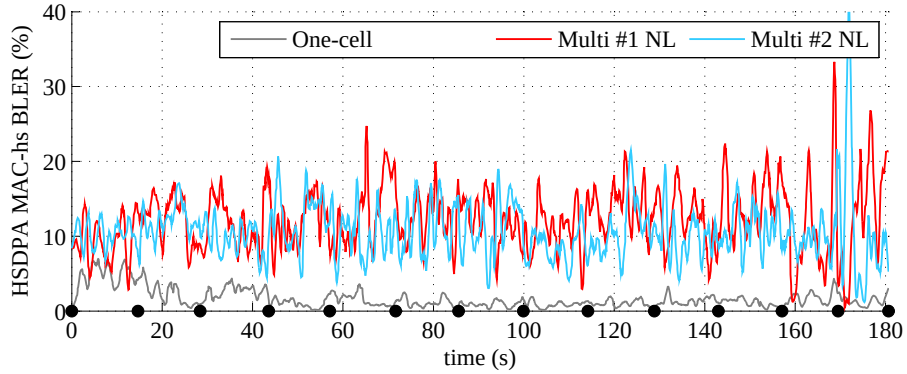

(c) BLER.

Figure L3.2 *Behavior of TBS, TP and BLER versus time in BR scenario under NL situation. Graphs have been smoothed in Matlab by means of a moving average of resolution 17. Lines plotted are the result of the combination of the four rounds performed for each measurement case. The points that appear at the bottom of the graph indicate the beginning of each route's row, i.e., markers 0, 3, 6, 9 and so on.*

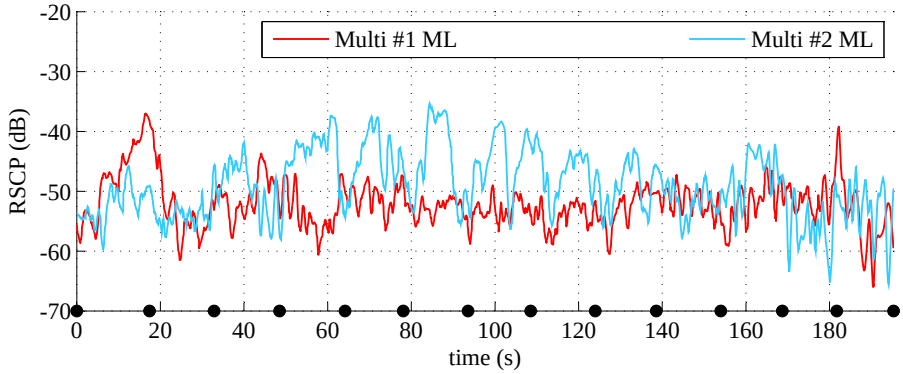

(a) *RSCP.*

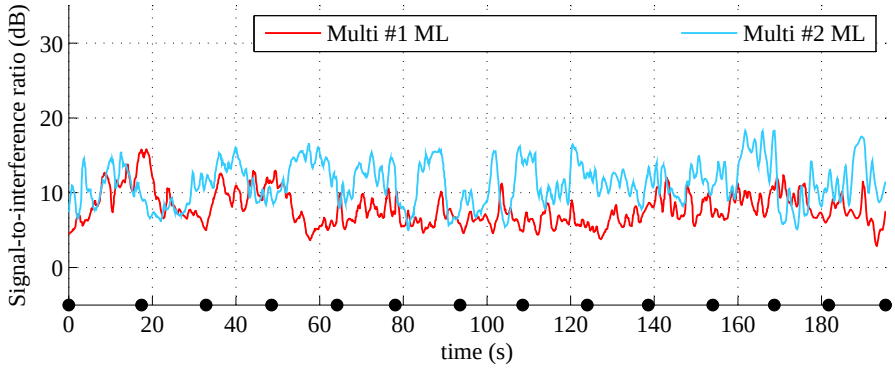

(b) *SIR.*

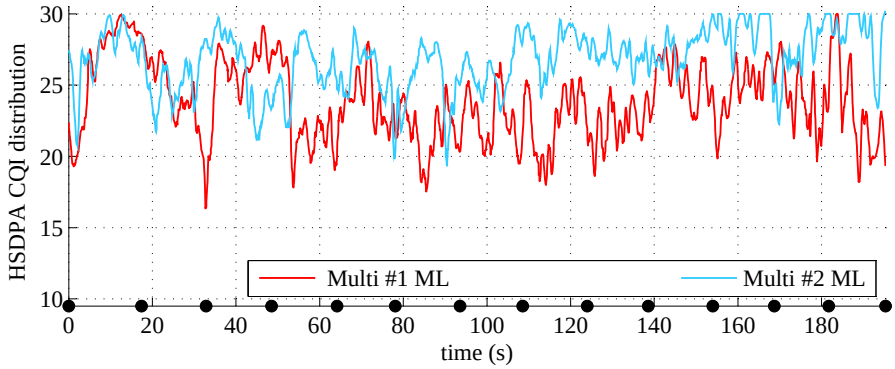

(c) *CQI.*

Figure L3.3 *Behavior of RSCP, SIR and CQI versus time in BR scenario under ML situation. Graphs have been smoothed in Matlab by means of a moving average of resolution 17. Lines plotted are the result of the combination of the four rounds performed for each measurement case. The points that appear at the bottom of the graph indicate the beginning of each route's row, i.e., markers 0, 3, 6, 9 and so on.*

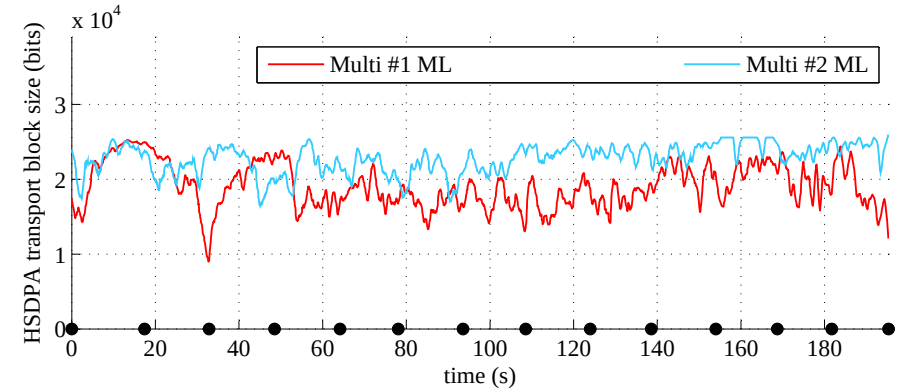

(a) TBS.

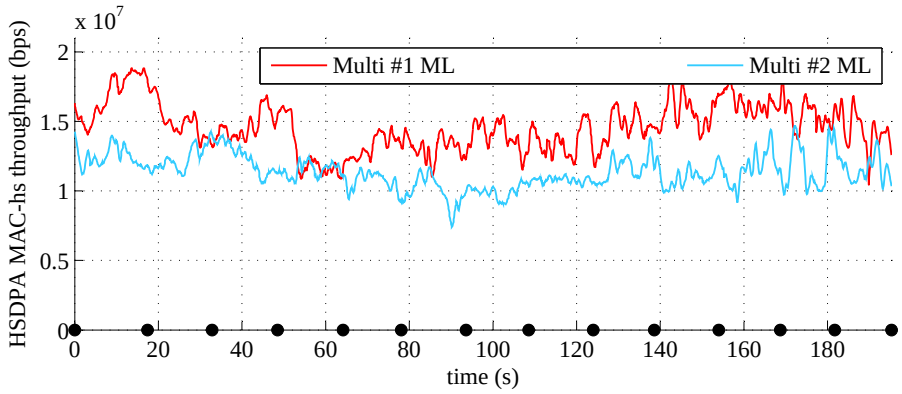

(b) System TP.

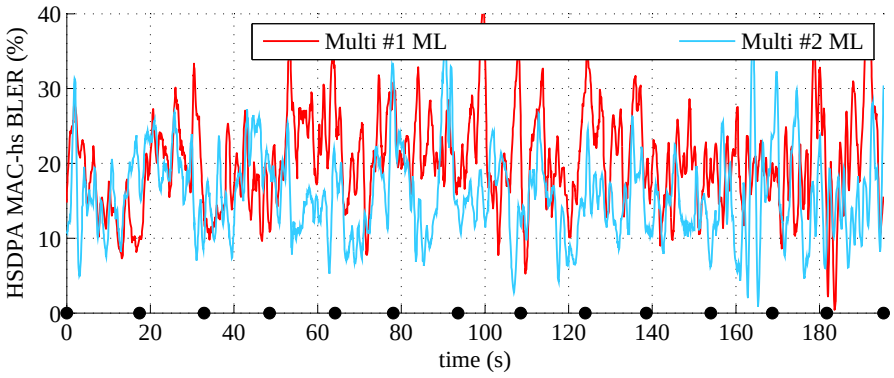

(c) BLER.

Figure L3.4 *Behavior of TBS, TP and BLER versus time in BR scenario under ML situation. Graphs have been smoothed in Matlab by means of a moving average of resolution 17. Lines plotted are the result of the combination of the four rounds performed for each measurement case. The points that appear at the bottom of the graph indicate the beginning of each route's row, i.e., markers 0, 3, 6, 9 and so on.*

APPENDIX D

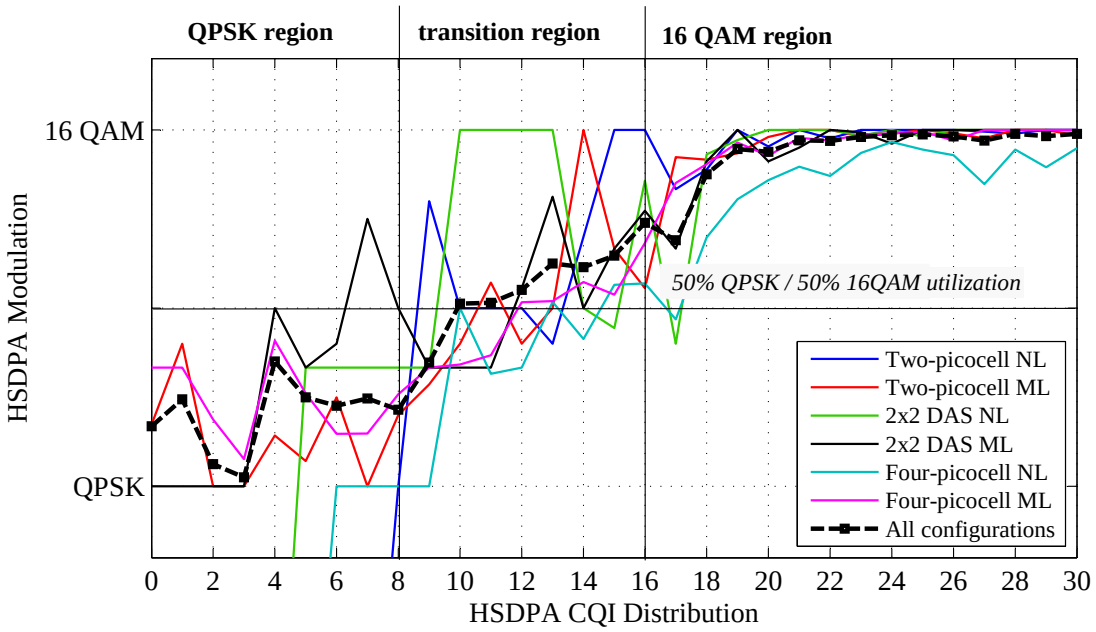

Figure L4.1 *Relation between modulation and CQI at HS scenario. For each CQI value, the ratio "(N-QPSK + 2xN-16QAM)/N is plotted, where N-QPSK and N-16QAM are the number of samples that reported QPSK and 16QAM usage respectively, and N is the total number of samples for that CQI value. For some CQI values no samples were gathered, and this is represented by zero values in the graph. "16 QAM region" is the CQI range where the 16 QAM utilization is more than 75 % and "QPSK region" is the CQI range where the QPSK utilization is more than 75 %. The "transition region" is in between those regions. Inaccuracies in the measurement software may produce this transition stage, where it can not be firmly stated the dominant modulation.*

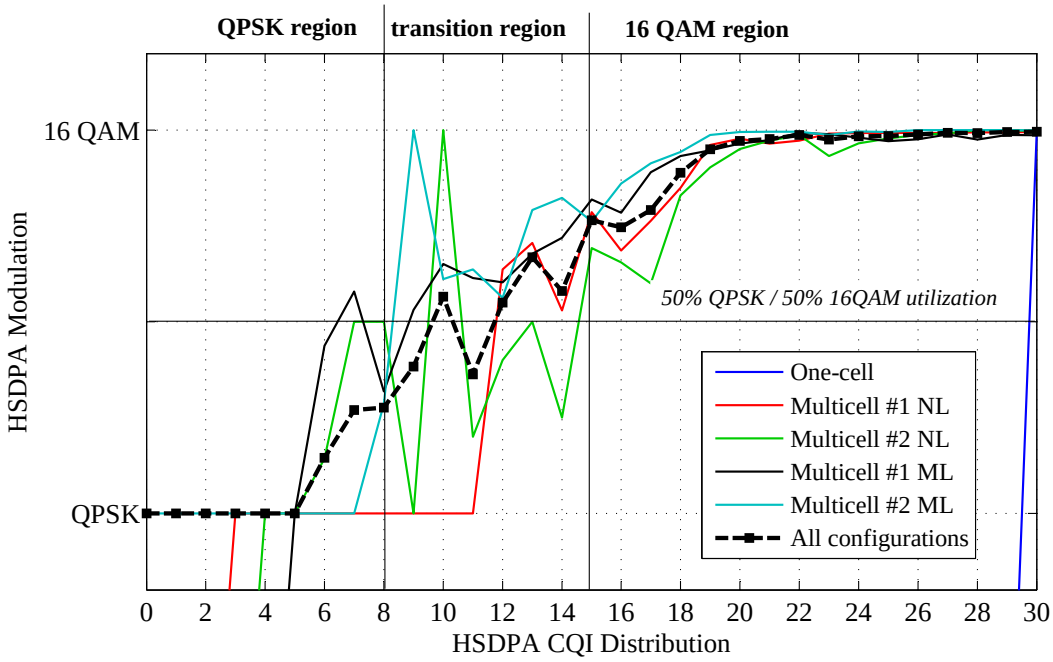

Figure L4.2 *Relation between modulation and CQI at BR scenario. For each CQI value, the ratio "(N-QPSK + 2xN-16QAM)/N is plotted, where N-QPSK and N-16QAM are the number of samples that reported QPSK and 16QAM usage respectively, and N is the total number of samples for that CQI value. For some CQI values no samples were gathered, and this is represented by zero values in the graph. "16 QAM region" is the CQI range where the 16 QAM utilization is more than 75 % and "QPSK region" is the CQI range where the QPSK utilization is more than 75 %. The "transition region" is in between those regions. Inaccuracies in the measurement software may produce this transition stage, where it can not be firmly stated the dominant modulation.*